1997

Investigation of the electrochemical behavior of ketorolac

Edward Kaiser
San Jose State University

INFORMATION TO USERS

This manuscript has been reproduced from the microfilm master. UMI films the text directly from the original or copy submitted. Thus, some thesis and dissertation copies are in typewriter face, while others may be from any type of computer printer.

The quality of this reproduction is dependent upon the quality of the copy submitted. Broken or indistinct print, colored or poor quality illustrations and photographs, print bleedthrough, substandard margins, and improper alignment can adversely affect reproduction.

In the unlikely event that the author did not send UMI a complete manuscript and there are missing pages, these will be noted. Also, if unauthorized copyright material had to be removed, a note will indicate the deletion.

Oversize materials (e.g., maps, drawings, charts) are reproduced by sectioning the original, beginning at the upper left-hand corner and continuing from left to right in equal sections with small overlaps. Each original is also photographed in one exposure and is included in reduced form at the back of the book.

Photographs included in the original manuscript have been reproduced xerographically in this copy. Higher quality 6" x 9" black and white photographic prints are available for any photographs or illustrations appearing in this copy for an additional charge. Contact UMI directly to order.

UMI

A Bell & Howell Information Company
300 North Zeeb Road, Ann Arbor MI 48106-1346 USA
313/761-4700 800/521-0600

INVESTIGATION OF THE ELECTROCHEMICAL BEHAVIOR OF KETOROLAC

A Thesis

Presented to the

Faculty of the Department of Chemistry

San Jose State University

In Partial Fulfillment

of the Requirements for the Degree

Master of Science

by

Edward Kaiser

May 1997

APPROVED FOR THE DEPARTMENT OF CHEMISTRY

Dr. Sam P. Perone

Dr. Craig Stone

Dr. Roger Biringer

APPROVED FOR THE UNIVERSITY

ABSTRACT

INVESTIGATION OF THE ELECTROCHEMICAL BEHAVIOR OF KETOROLAC

by Edward Kaiser

An experimental protocol was established for electrochemical (cyclic voltammetric) characterization of pharmaceutically important compounds where data would be suitable for subsequent multivariate analysis. As a prototype study, the electrochemical (cyclic voltammetric) behavior of the anti-inflammatory drug ketorolac was measured with a static mercury drop electrode (SMDE). A fractional factorial design was used to systematically study the effects of pH, analyte concentration, methanol concentration, scan rate, number of cycles and drop hang time. Signal-to-noise was significantly enhanced with the use of ensemble averaging and a Savitzky-Golay smoothing algorithm. The effects of the factors were assessed with peak current and peak potential values of the cyclic voltammograms. It was demonstrated that scan rate had a significant effect on the voltammetric data. The experimental results supported the proposed mechanism for similar pharmaceutically active compounds. This study demonstrates a useful protocol for acquiring meaningful voltammetric data from an electrochemically active pharmaceutical compound.

ACKNOWLEDGMENTS

My thanks and gratitude are extended to Professor Sam Perone for his constant support and encouragement. I would like to thank Professors Roger Biringer and Craig Stone for serving on the research committee. Dr. Joseph Muchowski from Roche Bioscience provided the pharmaceutical samples for use in these experiments and his support is appreciated. The financial assistance of my two employers Loral Space Systems and Dionex Corporation is gratefully acknowledged. In particular I would like to express my appreciation for technical assistance to Dr. Roy Okuda, Dong Qing Li and Joel Swanson from San Jose State University; Gary Grescek, Cynthia Nienart and Ron Wong from Princeton Applied Research; and Dr. John Statler and the Applications lab at Dionex Corporation. In addition, I would like to express my gratitude for the prayers and encouragement of the following family and friends: my parents Frank and Erika Kaiser, my sister Gloria Hale, Ilene Gatien, Eugene Todd, Joseph Thompson, Cathy Penberthy, Pat Stone, Scott Segelke, Joe and Heather Dody, and Linda Sherville.

TABLE OF CONTENTS

Page

I. Introduction 1

II. Biological Properties 2

A. Non-Steroidal Anti-Inflammatory Drugs 2

B. Ketorolac 3

C. Acute Assays 5

D. Cyclooxygenase Inhibition 5

E. Mechanism of Action 6

III. Experimental Section 9

A. Chemicals and Reagents 9

B. Apparatus 10

C. Electrochemical Measurements 11

D. Experimental Design 15

V. Results and Discussion 20

A. *iR* Compensation 20

B. Optimizing Voltammetric Parameters 23

C. Voltammetric Response Characteristics 30

D. Ensemble Averaging of Voltammetric Data 33

E. Data Smoothing of Voltammetric Data 33

F. Voltammetric Results 38

G. Evaluation of Variable Effects 52

H. Effect of Variables 65

1. Effect of Number of Cycles 70

Page

2. Effect of Switching Potential 70

3. Effect of Drop Hang Time 72

4. Effect of Analyte Concentration 72

5. Effect of Methanol Concentration 72

6. Effect of Scan Rate 73

7. Effect of pH 76

I. Electrochemical Mechanism 80

VI. Summary 88

VII. Conclusions 89

VIII. Bibliography 90

LIST OF TABLES

Table Page

1. Values for the Experimental Variables 16
2. Plackett-Burman Design Array 18
3. Modified Plackett-Burman Design Array 19
4. *iR* Compensation Feedback Parameters for Ketorolac Study 21
5. *iR* Compensation Results in Ohms 24
6. Setup Parameters for Cyclic Voltammetric Experiments 25
7. Experimental Design Voltammetric Results 50
8. Diffusion-Controlled Baseline Processing for Experiment 1' 51
9. Diffusion-Controlled Baseline Processing Results 54
10. Calculated Current Function $[i_p/ (v^{1/2} C^b)]$, for Cathodic Peaks A and B Voltammetric Data 56
11. Calculating the Effect of Scan Rate on Peak B Using Current Function $[i_p/ (v^{1/2} C^b)]$. 57
12. Summary of Factor Effects on Current Function $[i_p/ (v^{1/2} C^b)]$ for Peak B Voltammetric Data at pH 7 and 11 Using Voltammetric Data from Experiments 1' - 8' 58
13. Summary of Factor Effects on Current Function $[i_p/ (v^{1/2} C^b)]$ for Peak B Voltammetric Data at pH 6 and 7 Using Voltammetric Data from Experiments 1' - 4' and 5" - 8 " 59

Table Page

14. Summary of Factor Effects on Current Function $[i_p/ (v^{1/2} C^b)]$ for Peak A Voltammetric Data at pH 6 and 7 Using Voltammetric Data from Experiments 1' - 4' and 5" - 8" 60

15. Calculating Significance of the Scan Rate Factor Effect on Current Function $[i_p/ (v^{1/2} C^b)]$ Based on Peak B Voltammetric Data for pH 7 and 11 66

16. F-test Results for Factor Effects on Current Function $[i_p/ (v^{1/2} C^b)]$ Based on Peak B Voltammetric Data for pH 7 and 11, $F_c = 5.99$ 67

17. F-test Results for Factor Effects on Current Function $[i_p/ (v^{1/2} C^b)]$ Based on Peak B Voltammetric Data for pH 6 and 7, $F_c = 5.99$ 68

18. F-test Results for Factor Effects on Current Function $[i_p/ (v^{1/2} C^b)]$ Based on Peak A Voltammetric Data for pH 6 and 7, $F_c = 5.99$ 69

19. Peak Potential E_p for Varying Methanol Concentrations 75

20. Peak Potential E_p for Varying Scan Rates 77

21. Peak Potential E_p for Varying pH for Peak A 84

22. Peak Potential E_p for Varying pH for Peak B 85

LIST OF FIGURES

Figure Page

1. Structural formulas for ketorolac tromethamine, tolemetin sodium, and zomepirac sodium. 4

2. Important features of cyclooxygenase-mediated prostaglandin biosynthesis. 7

3. Basic features of the hypothesized fatty acid substrate binding site of prostaglandin synthetase with a structure of indomethacin (based on reference 28). 8

4. Cyclic voltammetry potential sweep, resultant reversible voltammogram, and resultant irreversible voltammogram. 12

5. Representative results for an *iR* compensation experiment. Conditions in Table 4. 22

6. Cyclic voltammogram for an irreversible reaction illustrating: initial potential (IP), peak potential (PP), vertex 1 potential (V1), and final potential (FP). 26

7. Comparison of high speed and high stability mode for acquiring voltammetric data for experiment 1'. Conditions in Table 3. 29

8. Representative analyte cyclic voltammogram for experiment 7'. Conditions in Table 3. 31

9. Representative blank cyclic voltammogram for experiment 7'. Conditions in Table 3. 32

10. Representative blank cyclic voltammogram for experiment 7' single run and ensemble-averaged for n=9. Conditions in Table 3. 34

Figure Page

11. Representative analyte cyclic voltammogram for experiment 7' single run and ensemble-averaged for n=9. Conditions in Table 3. 35

12. Blank cyclic voltammogram ensemble-averaged for n=9 for experiment 7' without smoothing and with 3 point Savitzky-Golay smoothing. Conditions in Table 3. 36

13. Analyte cyclic voltammogram ensemble-averaged for n=9 for experiment 7' without 3 point Savitzky-Golay smoothing and with 3 point Savitzky-Golay smoothing. Conditions in Table 3. 37

14. Detail of blank cyclic voltammogram for experiment 7' for single run, ensemble-averaged for n=9, and ensemble-averaged for n=9 with 3 point Savitzky-Golay smoothing. Conditions in Table 3. 39

15. Detail of analyte cyclic voltammogram using conditions for experiment 7' for single run, ensemble-averaged for n=9, and ensemble-averaged for n=9 with 3 point Savitzky-Golay smoothing. Conditions in Table 3. 40

16. Ensemble-averaged, smoothed and blank corrected analyte cyclic voltammogram for experiment 7'. Conditions in Table 3. 41

17. Ensemble-averaged, smoothed and blank corrected analyte cyclic voltammograms for experiment 1' and experiment 2'. Conditions in Table 3. 42

18. Ensemble-averaged, smoothed and blank corrected analyte cyclic voltammograms for experiment 3' and experiment 4'. Conditions in Table 3. 43

Figure Page

19. Ensemble-averaged, smoothed and blank corrected analyte cyclic voltammograms: experiment 5' and experiment 6'. Conditions in Table 3. 44

20. Ensemble-averaged, smoothed and blank corrected analyte cyclic voltammograms: experiment 7' and experiment 8'. Conditions in Table 3. 45

21. Ensemble-averaged, smoothed and blank corrected analyte cyclic voltammograms: experiment 5" and experiment 6". Conditions in Table 3. 46

22. Ensemble-averaged, smoothed and blank corrected analyte cyclic voltammograms: experiment 7" and experiment 8". Conditions in Table 3. 47

23. Ensemble-averaged, smoothed and blank-corrected analyte cyclic voltammograms for experiment 1' illustrating cathodic peak A, cathodic peak B, and reduction peak on anodic sweep A'. Conditions in Table 3. 49

24. Detail of experiment 1' blank-corrected analyte cyclic voltammograms processed to define diffusion-controlled baseline region (dotted line) for peak B. Conditions in Table 3. 53

25. Calculated factor effect on the current function $i_p/ (v^{1/2} C^b)$ for peak B at pH 11 and pH 7 for the seven factors: pH, analyte concentration, methanol concentration, scan rate, hang time, number of cycles, and switching potential using experiments 1' - 8'. 61

26. Calculated factor effects on the current function $i_p/ (v^{1/2} C^b)$ for peak B at pH 6 and pH 7 for the seven factors: pH, analyte concentration, methanol concentration, scan rate, hang time, number of cycles, and switching potential using experiments 1' - 4' and 5" - 8". 62

Figure Page

27. Calculated factor effects on current function $i_p/ (v^{½} C^b)$ for peak A at pH 6 and pH 7 for the seven factors: pH, analyte concentration, methanol concentration, scan rate, hang time, number of cycles, and switching potential using experiments 1' - 4' and 5" - 8". 63

28. Ensemble-averaged, smoothed and blank corrected analyte cyclic voltammograms for experiment 2' with cycle number noted. Conditions in Table 3. 71

29. Smoothed and blank corrected analyte cyclic voltammograms varying methanol concentration for experiment 7' run at 2.5% methanol and 10% methanol. Conditions in Table 3. 74

30. Smoothed and blank corrected analyte cyclic voltammograms varying scan rate for experiment 7' run at 250 mV/sec and 1000 mV/sec. Conditions in Table 3. 78

31. Effect of pH on voltammetric behavior using experiment 7' conditions (see Table 3). Voltammograms are blank-corrected for n=3. 79

32. Effect of pH on the peak potential E_p for ketorolac voltammetric data using experiment 7' conditions (see Table 3). 81

33. Effect of pH on the peak current i_p for ketorolac voltammetric data using experiment 7' conditions (see Table 3). 82

34. Smoothed and blank corrected analyte cyclic voltammograms varying pH for experiment 7' run at pH 6 and pH 7. Conditions in Table 3. 83

35. Proposed mechanism for the reduction of ketorolac tromethamine based on reference 67. 87

I. Introduction

Considerable effort and expense are directed toward the development of any new pharmaceutical compound. A drug company typically will spend 10 or more years to study and test a new drug before the Food and Drug Administration (FDA) approves it for marketing and general use. A drug development team of pharmacists, medical personnel, statisticians, toxicologists, and chemists is needed to generate and analyze an enormous amount of data. Estimates of the total development cost for each drug that reaches the US market range from $125-230 million (1, 2).

Drug companies want to invest their research funds as efficiently as possible for pharmaceutical development. They cannot afford a policy of developing drugs by random chance or by accident, although many valuable pharmaceutical compounds have indeed been discovered in this manner. It is far better to use the vast body of chemical knowledge and inherent structure-property relationships as a guide to systematic drug development.

Electrochemistry is a useful research tool for investigating drugs and pharmaceuticals that are electroactive. A variety of techniques have been utilized: amperometry, conductometry, coulometry, ion-selective electrodes, potentiometry, voltammetry, stripping voltammetry (anodic and cathodic), and liquid chromatography-electrochemistry (3-5). Analytical methods based on these techniques have been developed to monitor the quality of drugs manufactured as well as determining concentrations in physiological fluids for clinical applications. Electrochemical techniques have also been employed to study the mechanism of drug activity.

Previous studies of the information content of voltammetric data for a variety of electrochemically active compounds have demonstrated that pattern recognition can be used to identify multiplets (6), classify electrode processes (7) and identify herbicidal activity of nitrodiphenyl ethers (8). These previous investigations suggested that the same approach could be used to investigate electrochemically active pharmaceutical compounds.

The goal of this investigation was to develop an experimental protocol with which to characterize the voltammetric properties of pharmaceutically important compounds so that correlation between voltammetric properties and pharmacological activity might be investigated with valid and reproducible electrochemical data. For this study, ketorolac, an anti-inflammatory drug, was selected as the representative pharmaceutical compound.

II. Biological Properties

A. Non-Steroidal Anti-Inflammatory Drugs

Ketorolac is a compound from a class of pharmaceutical compounds known as nonsteroidal anti-inflammatory drugs (NSAIDs). These drugs have long been used as an analgesic for the treatment of minor pain as well as for the treatment of inflammation and fever. Aspirin is a well-known example of an NSAID that has been used since the 1880s.

NSAIDs can be separated by their structures into groups that include salicylates and arylacetic acids (9). Aspirin is a member of the salicylate group. Arylacetic acids and related compounds comprise the other group of NSAIDs that have become very important drugs for the treatment of pain and inflammation. The common structural features of these compounds are an acetic acid side-chain attached to a benzoid or heteroaromatic ring.

features of these compounds are an acetic acid side-chain attached to a benzoid or heteroaromatic ring.

Arylacetic acids and related compounds have a broad range of functions in the treatment of pain and inflammation. Ibuprofen [α-Methyl-4-(2-methylpropyl)-benzenacetic acid, Motrin] is used for the temporary relief of minor aches and pains associated with the common cold, headache, toothache, muscular aches, backache, for the minor pain of arthritis, for the pain of menstrual cramps and for the reduction of fever (10). Tolmetin sodium [1-methyl-5-(4-methylbenzoyl)-1H-pyrrole-2-acetic acid, Tolectin] is effective in treating the symptoms of rheumatoid arthritis, osteoarthritis and juvenile rheumatoid arthritis (11, 12). Naproxen [(+) 6-Methyoxy-α-methyl-2-napth-alene-acetic acid, Naprosyn] is used for the treatment of rheumatoid arthritis, osteoarthritis, ankylosing spondylitis, tendinitis, bursitis, and acute gout (13).

B. Ketorolac

Ketorolac is an arylacetic acid NSAID with potent analgesic and moderate anti-inflammatory activity. Administered as a tromethamine salt, ketorolac is sold as tablets and in an injectable form for post-operative use. More than 16 million patients have used ketorolac in 28 countries. It has been shown to give essentially equivalent performance to morphine for the relief of post-operative pain without undesirable side effects (14, 15).

Ketorolac was developed at Roche Bioscience in Palo Alto, California [formerly Syntex Inc.] in the early 1970s (16, 17). It is structurally related to tolmetin and zomepirac, two pyrroleacetic acid derivatives (see Figure 1). Ketorolac exhibited the

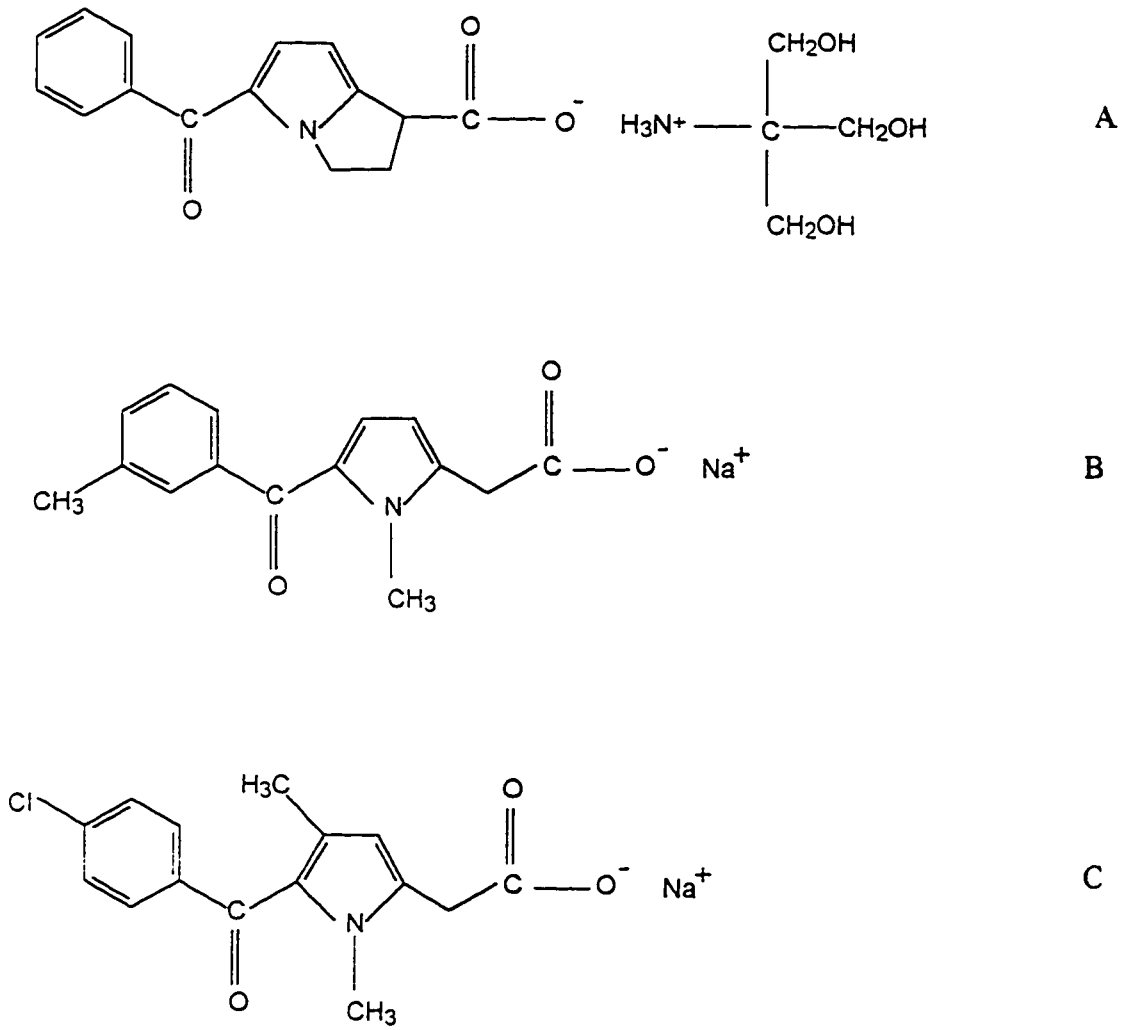

Figure 1. Structural formulas of ketorolac tromethamine (A), tolemetin sodium (B), and zomepirac sodium (C).

highest anti-inflammatory activity but with a minimum of side effects out of a pool of 120 related compounds.

C. Acute Assays

Ketorolac analogs were assayed for anti-inflammatory and analgesic activity with rats. A drug's anti-inflammatory activity describes its ability to reduce inflammation, characterized by redness, swelling and heat. Anti-inflammatory potency for ketorolac was measured by the inhibition of the carrageenan-induced edema assay (18-20). Analgesic activity refers to a drug's ability to reduce pain. This was measured by the inhibition of the phenylquinone-induced writhing assay (21). Both of these are standard tests that have been used in previous investigations of other related pharmaceutical compounds.

D. Cyclooxygenase Inhibition

NSAID function was discovered in 1971, when Vane reported that aspirin blocks the synthesis of prostaglandins (22). Prostaglandins are physiologically active compounds formed from essential fatty acids. The activities of these compounds affect physiological processes such as contraction of smooth muscle, blood pressure, nerve transmission, water retention, electrolyte balance, and blood clotting (23). The structure of prostaglandins is based on a C_{20} polyunsaturated fatty acid containing an internal cyclopentane ring. Research on these compounds is difficult because prostaglandins are present in low concentrations (10^{-9} g or less) and can degrade quickly.

Prostaglandin synthesis begins with arachidonic acid (5,8,11,14-eicosatetraenoic acid), a major C_{20} polyunsaturated acid. An enzyme complex called cyclooxygenase (or

fatty acid dioxygenase) catalyzes the reaction of arachidonic acid by oxidation and cyclization to 15-hydroperoxy-9,11-peroxidoprosta-5,13-dienoic acid (PGG_2), a precursor to various prostaglandins (Figure 2). An inhibitor is a compound that stops or slows down the activity of an enzyme. This is accomplished by preventing the formation or productive breakdown of either the enzyme-substrate or enzyme-product complexes.

E. Mechanism of Action

NSAIDs inhibit the first step of the prostaglandin synthesis process to provide relief from pain and inflammation (9). In 1964, Shen proposed a receptor site model for the PG synthetase enzyme (24). Based on the results of this study the structure of indomethacin and other NSAIDs can be correlated to their ability to bind to the active site.

A variety of mechanisms have been proposed to describe the binding site used by these pharmaceutical agents. Gund and Shen suggested a complementary receptor site model based on conformational analysis of indomethacin and other non-steroidal anti-inflammatory drugs (25). Initially the carboxyl group binds by hydrogen or coulombic bonding to anchor the substrate. The rest of the molecule is then folded onto the active site where the saturated ring structure is accepted into a broad hydrophobic region. Finally the aromatic group fits into a hydrophobic groove. Figure 3 illustrates the basic features of the hypothesized binding site with a structure of the indomethacin molecule (26).

Though few details have been published concerning the mechanism of ketorolac's analgesic and anti-inflammatory activity (27), the above mentioned features of the inhibition mechanism of other NSAIDs can be applied to ketorolac. Of particular interest

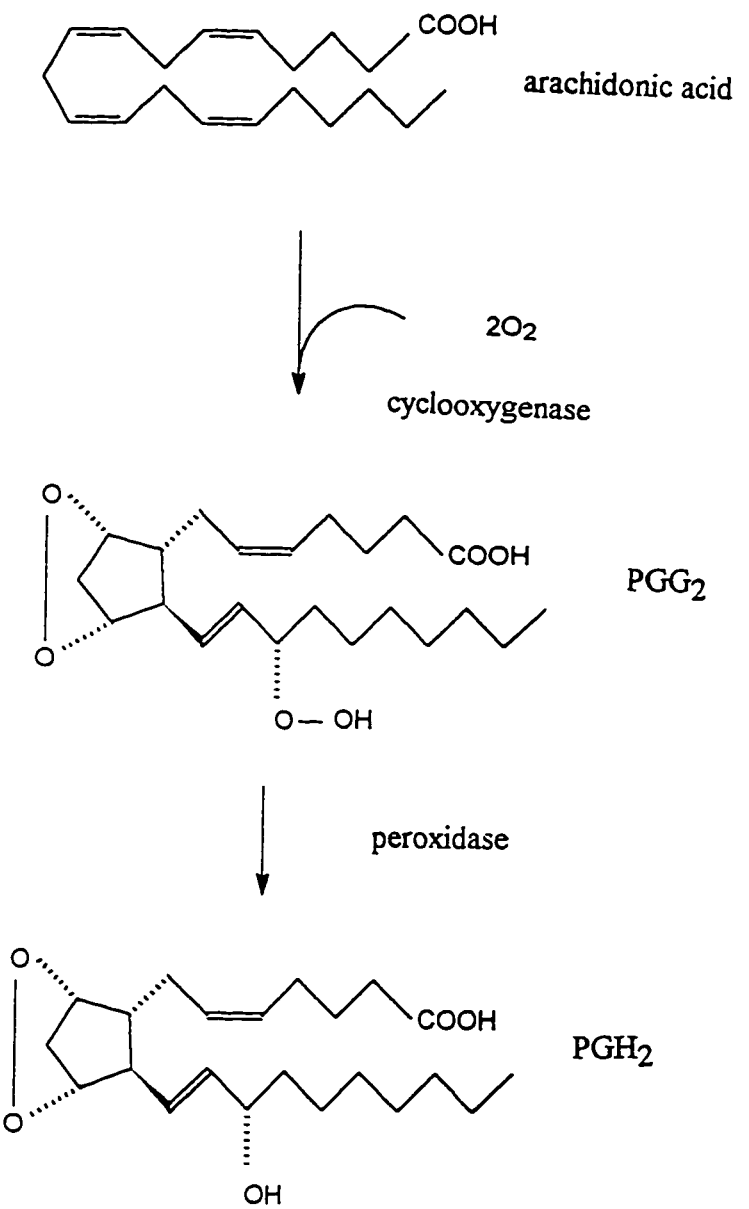

Figure 2. Important features of the cyclooxygenase-mediated prostaglandin biosynthesis.

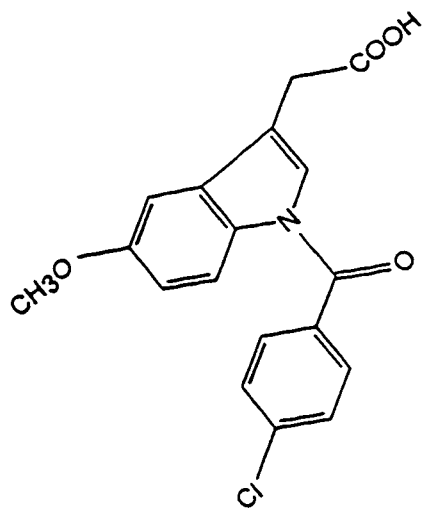

Indomethacin

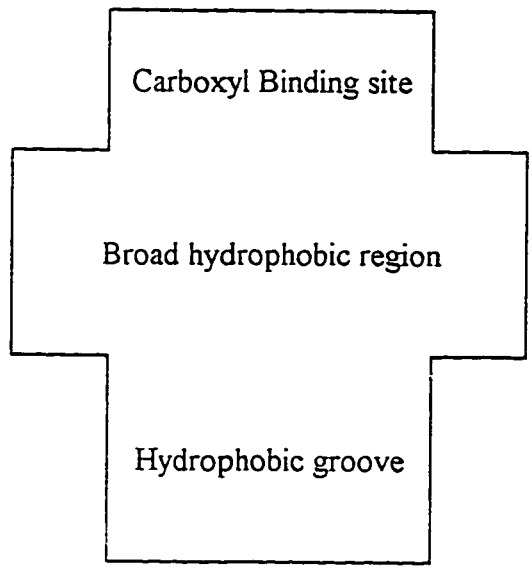

Figure 3. Basic features of the hypothesized fatty acid substrate binding site of prostaglandin synthetase with a structure for indomethacin (based on reference 28).

to this study is the role of the carbonyl compound. There are examples of NSAIDs in which anti-inflammatory activity diminishes but is not eliminated when a CH_2 group replaces the carbonyl group (28). This suggests that it is not directly involved in anti-inflammatory activity.

III. Experimental Section

A. Chemicals and Reagents

All chemicals were reagent grade and were used as received. Double-distilled water was used for preparing all solutions. The pharmaceutical compound ketorolac tromethamine [(±)-5-benzoyl-2,3-dihydro-1H-pyrrolizine-1-carboxylic acid, 2-amino-2-hydroxymethyl-1,3-propanediol] was obtained from Roche Bioscience in Palo Alto, CA, USA [formerly Syntex Inc.] and was used without further purification. A stock solution of this compound (0.02 M) was prepared in high purity methanol (Fisher Scientific, Fair Lawn, NJ) and was stored at 5° C when not in use. Fresh standard solutions were prepared every two weeks.

Working solutions of the analyte were prepared by diluting the stock solution with a Britton-Robinson buffer to a final volume. This buffer was prepared by adding reagent grade boric acid, sodium acetate, dibasic potassium phosphate and potassium chloride so that each of the components was 0.02 F (8). The Britton-Robinson buffer solutions were diluted to a final volume using double distilled water and high purity methanol at two concentrations: 10 % and 2.5 % methanol. The pH of the buffer was adjusted to a pH of 6, 7, or 11 with 0.2 M sodium hydroxide or 0.2 M sulfuric acid. Buffer solutions were

prepared fresh daily.

B. Apparatus

Electrochemical measurements were made with an EG&G PAR (Princeton, NJ, USA) Model 273 Potentiostat/Galvanostat equipped with a Model 303A Static Mercury Drop Electrode (SMDE). The working electrode consisted of a small size SMDE with a nominal area of 0.96×10^{-2} cm^2 (29). An EG&G PAR capillary assembly with a 0.16 mm i.d. (P/N G0198) was used to dispense mercury from the reservoir of the electrode assembly. The capillary was stored in a container of mercury when not in use. A platinum wire served as the counter electrode.

All potentials were measured and reported versus a Ag / AgCl / saturated KCl / saturated AgCl reference electrode. A EG&G PAR AgCl-KCl filling solution (P/N RDE0022) was used as the reference electrode solution. For the EG&G PAR reference electrode jacket (P/N G0159) a Vycor frit with Teflon heat-shrink tubing (P/N G0100) was used. The frit was changed periodically according to the manufacturer's recommendation. The reference electrode was stored in the reference electrode filling solution when not in use.

The potentiostat was controlled by an IBM/486 compatible computer with an EG&G PAR Model 307 Interface Accessory. A GPIB (IEEE-488) instrumentation data bus was used for data transfer between the electrochemical instrumentation and the computer. EG&G PAR Model 270 Electrochemical Analysis Software version 4.11 was employed for data acquisition and instrument control. Replicate electrochemical experiments were run with the Autoexecute feature in the software.

C. Electrochemical Measurements

Potentials for electrochemical data were corrected for *iR* drop. It is necessary to take into consideration the resistance between the working electrode surface and the reference electrode otherwise there would be an error in measuring the true potential at the working electrode (30). A positive feedback algorithm in the electrochemical software was utilized to correct for the *iR* drop prior to running an electrochemical experiment. This technique is recommended for fast acquisition rates (31). By using a feedback of the output of the current-measuring amplifier to the input of the potentiostat-controlled amplifier it was possible to correct for up to 85% of the uncompensated resistance (32).

Cyclic voltammetry was chosen to study ketorolac because it can be used to give insight about the mechanism of electrochemical reactions (33-35). In this technique an applied potential is swept linearly to a specific peak over a specified range and then decreased to its starting point at the same rate. A representative voltage sweep is shown in Figure 4A. The data points that were collected were presented as a voltammogram with current plotted on the y-axis and voltage on the x-axis. Figure 4B shows a representative voltammogram for a "reversible" reaction. The top portion of the voltammogram from the start of the sweep to the switching potential is the cathodic peak in which the analyte A is reduced.

$$A + e \rightarrow A^{\cdot -} \qquad (1)$$

The analyte becomes reoxidized and the resultant anodic peak occurs.

$$A^{\cdot -} - e \rightarrow A \qquad (2)$$

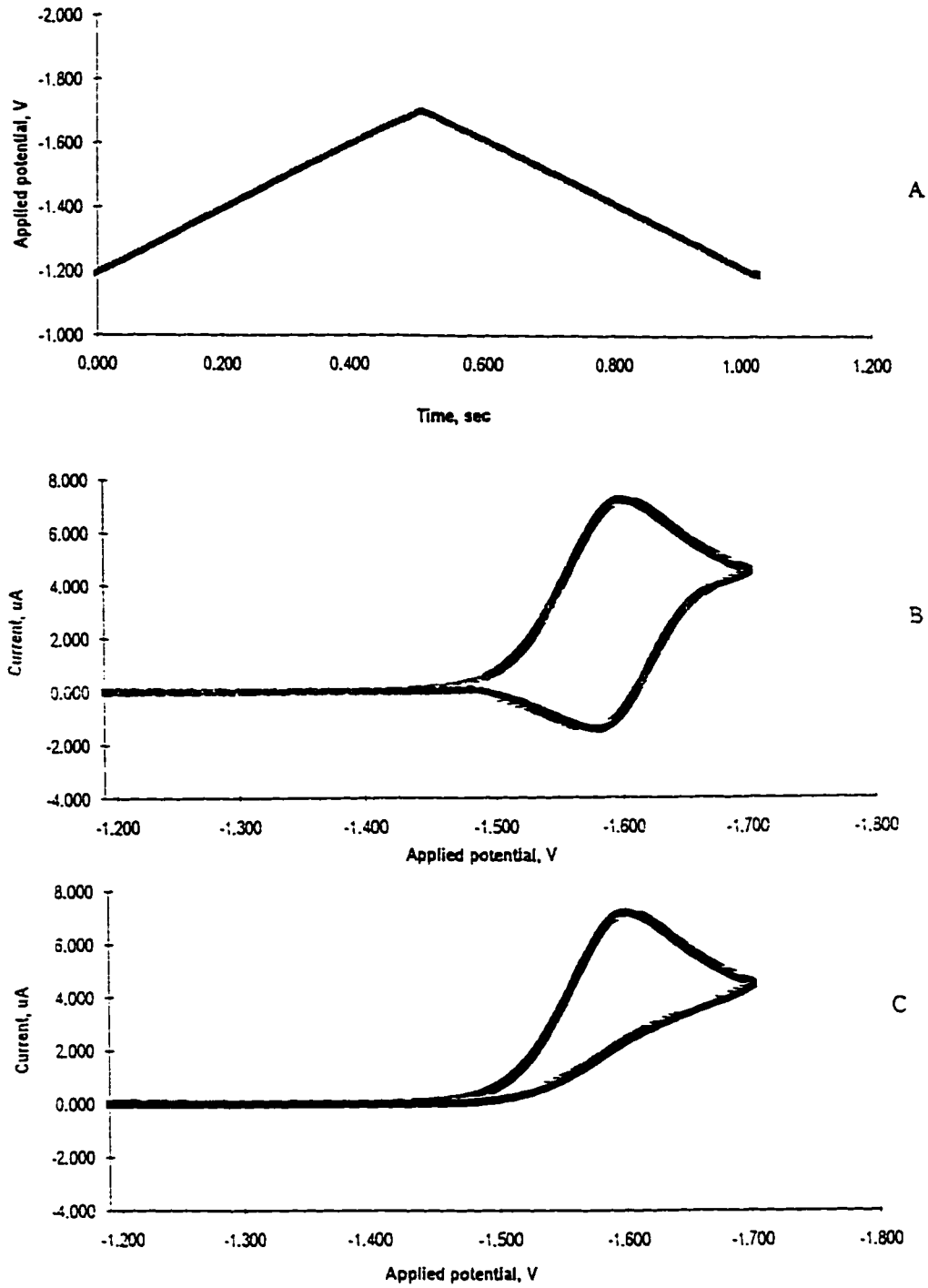

Figure 4. Cyclic voltammetry potential sweep (A), resultant reversible voltammogram (B), and resultant irreversible voltammogram (C).

If the product that is formed in the cathodic peak is not reoxidized at a significant rate on the reverse scan then an anodic peak is not observed. An example of an "irreversible" reaction is shown in Figure 4C.

Voltammograms were ensemble averaged to enhance signal-to-noise ratios (36, 37). The electrochemical software in the File Math portion of the Numeric menu permitted summing successive voltammograms point by point. The summed data were subsequently divided by the number of voltammograms used. In this study, nine replicate voltammograms were used for ensemble averaging. The benefit of this technique is that the random noise in the voltammograms is diminished by a factor of $1/n^{½}$, where n is the number of cycles. Both standard and blank runs were ensemble averaged for n=9 except where noted.

Further improvement in the quality of the data was accomplished by use of a data smoothing software algorithm. The EG&G PAR software allows selection between two different smoothing algorithms: Moving (or Sliding) Average and Savitzky-Golay. The Moving Average operates on a moving data window of a specified number of points, adds their y-values and then replaces the midpoint with the average value. The Savitzky-Golay smoothing algorithm functions by replacing the center point of a data point sequence with a point based on a polynomial equation selected to describe that data set (38).

The Savitzky-Golay smoothing function was selected for this work because it was found to be better at minimizing the effect of short term random noise without affecting the analytical signal. The Moving Average routine is good at minimizing noise but has the

disadvantage of degrading peak intensity (39). Three different data windows are available for the Savitzky-Golay smoothing function: linear (3 point), quadratic (5 point) or cubic (7 point). The algorithm works by considering a group of points, eliminating the leftmost point and adding a new point on the right. The linear (3 point) data window was selected because it best matched the character of the short term spikes found in the voltammetric data.

All voltammograms were blank corrected. This was accomplished by preparing electrochemical blank test solutions identical to the analytical runs except without the presence of the analyte. The blank voltammetric data were also subjected to the same data processing mentioned earlier [ensemble averaging for n=9 followed by the Savitzky-Golay linear (3 point) smoothing]. To blank correct, the smoothed/ensemble averaged blank voltammogram was subtracted point for point from the smoothed/ensemble averaged analytical voltammogram run under the same conditions. This was accomplished by using the file subtraction feature in the electrochemical software.

All measurements were performed at room temperature (28 ± 1.0 °C). To diminish the influence of dissolved oxygen, all solutions were purged with high-purity nitrogen for a minimum of four minutes before each electrochemical measurement was recorded. The nitrogen used was passed through a solution of the same composition as the supporting electrolyte in order to saturate the nitrogen with solvent vapor. Voltammetry was conducted in EG&G PAR borosilicate glass cells (P/N G0057) with a working volume of 3 to 20 mL.

D. Experimental Design

To maximize the amount and accuracy of information that was received from a given set of experimental runs, a planned sequence of experiments linking changes in input variables with changes in voltammetric behavior was designed. This experimental design facilitated the study of how responses change and interact at different variable settings. Seven variables were selected for investigation: pH, analyte concentration, methanol concentration, scan rate, number of cycles, drop hang time, and switching potential. The first three are solution variables and the last four are electrochemical variables. A low and high level for each of the variables was selected based on a previous study (40). Two sets of experiments were conducted using two different pairs of pH values, see Table 1. Two variables (number of cycles and switching time) were considered dummy variables (41) when evaluating factor effects on the first cathodic sweep. These were used as an estimate for the variance of the system. There should be no change detected in the properties of the voltammetric peaks exhibited in the first cathodic sweep for the high and low values of the dummy variables.

A limited number of experiments were performed due to cost and sample supply considerations. A full factorial design in which all possible combinations of the seven factors are investigated would have required 2^7 or 128 runs. To conduct such an investigation would have been cost prohibitive. Also, some of the pharmaceutical compounds that will be used in further investigations were in limited supply (for one compound less than 100 milligrams was available).

Table 1. Values for the Experimental Variables

A. Experiment Set I

Variable no.	Variables	Low	High
X_1	pH	11	7
X_2	Analyte conc.	0.1 mM	0.5 mM
X_3	MeOH conc.	2.5 %	10.0 %
X_4	Scan rate	250 mV/sec	1000 mV/sec
X_5	# cycles	1 (1 mV/pt)	2 (2 mV/pt)
X_6	Drop hang time	1 s	30 s
X_7	Switching potential	50 mV	100 mV

B. Experiment Set II

Variable no.	Variables	Low	High
X_1	pH	7	6
X_2	Analyte conc.	0.1 mM	0.5 mM
X_3	MeOH conc.	2.5 %	10.0 %
X_4	Scan rate	250 mV/sec	1000 mV/sec
X_5	# cycles	1 (1 mV/pt)	2 (2 mV/pt)
X_6	Drop hang time	1 s	30 s
X_7	Switching potential	50 mV	100 mV

Use of a fractional factorial design for this study minimized the number of experiments while maintaining maximum precision (42). With this design, only the most important interactions are tested. Aliasing refers to a situation in the full factorial experiment where identical interactions exist. In the fractional factorial experiment these are eliminated. This loss of redundancy results in fewer tests yet with a reasonable estimate for the important interactions of the factors of interest.

A two-level fractional factorial Plackett-Burman design was selected for this study (43). These are designs for studying K = N-1 factors in N runs, where N is a multiple of 4. In this study, K = seven (for seven factors) with N = eight (for eight runs). Table 2 lists the experimental settings for the Plackett-Burman array that were utilized. The order of the experiment number was changed to indicate the actual sequence in which experiments with similar conditions were run, as shown in Table 3. This design is balanced because each factor is run the same number of times at the high and low levels (44). This can be verified by the fact that there is an equal number of (+) and (-) values in each column and row.

A balanced design simplifies the statistical calculations. It can be assumed that the variances for both the high and low values are the same since their sample sizes are the same. This would not be the case if the sample sizes were different. A two level design matrix that has vertical and horizontal balancing is orthogonal. Consequently, the average response from each column has the same influence on the evaluation of any effect. This allows the desired effects to be evaluated independently.

Table 2. Plackett-Burman Design Array

		Factors						
Original Experiment no.	**Modified Experiment no.**	X_1	X_2	X_3	X_4	X_5	X_6	X_7
1	1'	+	-	-	+	-	+	+
2	3'	+	+	-	-	+	-	+
3	4'	+	+	+	-	-	+	-
4	6'	-	+	+	+	-	-	+
5	2'	+	-	+	+	+	-	-
6	5'	-	+	-	+	+	+	-
7	8'	-	-	+	-	+	+	+
8	7'	-	-	-	-	-	-	-

note: "+" = high value, "-" = low value for each factor

Table 3. Modified Plackett-Burman Design Array

A. Experiment Set I

Modified Experiment no.	X_1	X_2	X_3	X_4	X_5	X_6	X_7
	pH	**Analyte Conc.**	**MeOH Conc.**	**Scan mV/s**	**# cyc.**	**Hang Time sec**	**Switch (E_{sw}-E_p) mV**
1'	pH 7	0.1 mM	2.5 %	1000	1	30	100
2'	pH 7	0.1 mM	10.0 %	1000	2	1	50
3'	pH 7	0.5 mM	2.5 %	250	2	1	100
4'	pH 7	0.5 mM	10.0 %	250	1	30	50
5'	pH 11	0.5 mM	2.5 %	1000	2	30	50
6'	pH 11	0.5 mM	10.0 %	1000	1	1	100
7'	pH 11	0.1 mM	2.5 %	250	1	1	50
8'	pH 11	0.1 mM	10.0 %	250	2	30	100

B. Experiment Set II

	pH	**Analyte Conc.**	**MeOH Conc.**	**Scan mV/s**	**# cyc.**	**Hang Time sec**	**Switch (E_{sw}-E_p) mV**
5"	pH 6	0.5 mM	2.5 %	1000	2	30	50
6"	pH 6	0.5 mM	10.0 %	1000	1	1	100
7"	pH 6	0.1 mM	2.5 %	250	1	1	50
8"	pH 6	0.1 mM	10.0 %	250	2	30	100

V. Results and Discussion

A. *iR* Compensation

The parameters for the *iR* experiment that were chosen are listed in Table 4 (45). A current range of 1 mA was selected because the largest peak current expected for the experimentation would not exceed this value. At this range the maximum resistance that can be offset is 2 kΩ, with a resolution of 1 Ω. The potential value of -1.400 V was selected because no electrochemical reaction occurs at the test conditions. It was not possible to compensate for all of the potential error so a compensation level of 85% was selected to avoid the phenomenon of high frequency oscillation or "ringing". The default value of 0.025 V was used as the pulse height and the resulting current waveform was monitored. The undershoot refers to how much oscillation in the applied potential that will be tolerated. The default value of 10% was utilized.

The rise time sets the bandwidth of the potentiostat. This is a measure of how quickly the instrument can respond to a change in the applied potential. There are two options available: high speed and high stability. With the high speed setting the instrument has a high bandwidth and can respond quickly but can be prone to oscillations. In the high stability mode this is less likely to occur. For this study the "high speed" mode gave the best results.

The result of a representative *iR* compensation experiment is shown in Figure 5. At least three replicate *iR* compensation experiments were conducted prior to analysis with the cell filled with the solution to be analyzed. The average resistance value for the uncompensated resistance was entered into the parameters required for the cyclic

Table 4. *iR* Compensation Feedback Parameters for Ketorolac Study

Current range	1 mA
Correction range	2 kΩ
Resolution	1 Ω
Potential value	-1.400 V
Compensation height	85%
Pulse height	0.025 V
Undershoot	10%
Rise time	High Speed

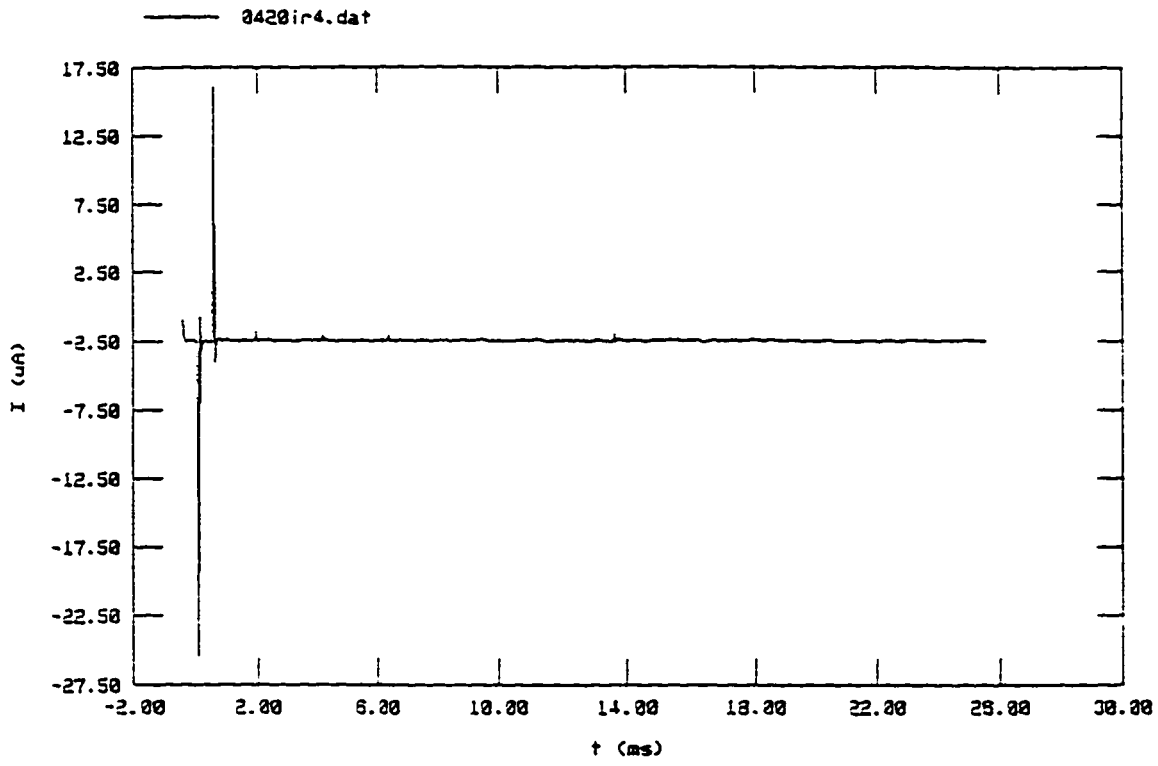

Remaining Uncompensated Resistance (RUR)	97.7 Ω
Compensated Portion of the Uncompensated Resistance (RU)	550.0 Ω
Estimated Total Uncompensated Resistance (RUT)	647.7 Ω

Figure 5. Representative results for an *iR* compensation experiment. Conditions in Table 4.

voltammetric experiment and are then subsequently used to automatically correct the applied potential for the measured current. The Uncompensated Resistance (RU) is the maximum uncompensated resistance that the software can compensate with the selected compensation and undershoot settings. RU values ranged from 452.3 to 734.4 Ω. Results for the *iR* compensation measurements are summarized in Table 5.

B. Optimizing Voltammetric Parameters

A variety of parameters were setup in the electrochemical software for the cyclic voltammetric experiments as summarized in Table 6 (46). The potential sweep was specified by means of an initial potential (IP), a peak potential (PP), a switching potential for the first segment or vertex 1 potential (V1), and a final potential (FP). It was possible with the software to specify all the parameters except the peak potential prior to running the experiment. The peak potential was determined after the run. Figure 6 illustrates how these values relate to the voltammogram for an irreversible reaction.

The voltammogram parameters were chosen so that the voltammetric data would be suitable for subsequent fast Fourier transformation (FFT) analysis (47). FFT is a mathematical function that takes the original signal in the time domain and converts it to one in the frequency domain. This technique has been proven beneficial to a variety of analytical technique to enhance signal-to-noise ratio. It has application to this study because it facilitates extracting features from each voltammogram. A requirement of the data set for FFT analysis is that the number of data points be equal to a product of prime factors such as 2, 3, 5, or 7 (48).

Table 5. *iR* Compensation Results in Ohms

Experiment number	Estimated Total Uncompensated Resistance (RUT)	Corrected Portion of Uncompensated Resistance (RU)	Remaining Uncompensated Resistance (RUR)
1'	661.5 ± 5.9	560.8 ± 4.3	101.0 ± 1.9
2'	785.4 ± 68.4	694.5 ± 61.9	124.2 ± 10.2
3'	661.3 ± 7.0	560.5 ± 6.4	100.4 ± 1.4
4'	857.0 ± 11.9	727.0 ± 9.6	130.0 ± 2.4
5'	590.6 ± 6.9	498.7 ± 4.7	91.91 ± 4.26
6'	858.9 ± 1.2	728.8 ± 2.1	130.1 ± 0.9
7'	533.4 ± 3.1	452.3 ± 3.1	81.11 ± 1.01
8'	866.4 ± 24.5	734.4 ± 21.9	132.4 ± 3.0
5''	681.7 ± 1.3	578.0 ± 0.0	103.7 ± 1.3
6''	747.7 ± 1.9	634.8 ± 1.5	112.9 ± 1.5
7''	632.7 ± 3.1	537.0 ± 2.8	95.7 ± 0.3
8''	783.1 ± 88.1	664.3 ± 76.2	118.8 ± 11.9

Table 6. Setup Parameters for Cyclic Voltammetric Experiments

Parameter	**Description**	**Units**
Initial potential (IP)	Potential applied at start of experiment	volt (V)
Final potential (FP)	Potential applied at start of experiment	volt (V)
Vertex 1 Potential (V1)	Ending potential of the 1st segment	volt (V)
Equilibration Time (ET)	Delay after drop has been dispensed	second (s)
Acquisition Mode (AM)	How many times the current is sampled (1/4, 2/4, 3/4, 4/4, All, Ramp)	-
Current range (CR)	Maximum current measured	amps (A)
Rise Time(RT)	Bandwidth characteristics of potentiostat (High Stability or High Speed)	-
Filter (FL)	Low-pass cut-off filter (Off, 5.3 Hz or 590 Hz)	-
iR Compensation (IR)	Apply *iR* compensation value	ohms (Ω)
Scan increment (SI)	Potential change per data point	millivolt (mV)
Scan rate (SR)	How quickly potential changes	volt/sec (V/s)
Step time (ST)	How long each scan increment is applied	second (s)
Number of points (NP)	Number of data points collected	-
Number of Cycles (NC)	The number of potential cycles performed	-

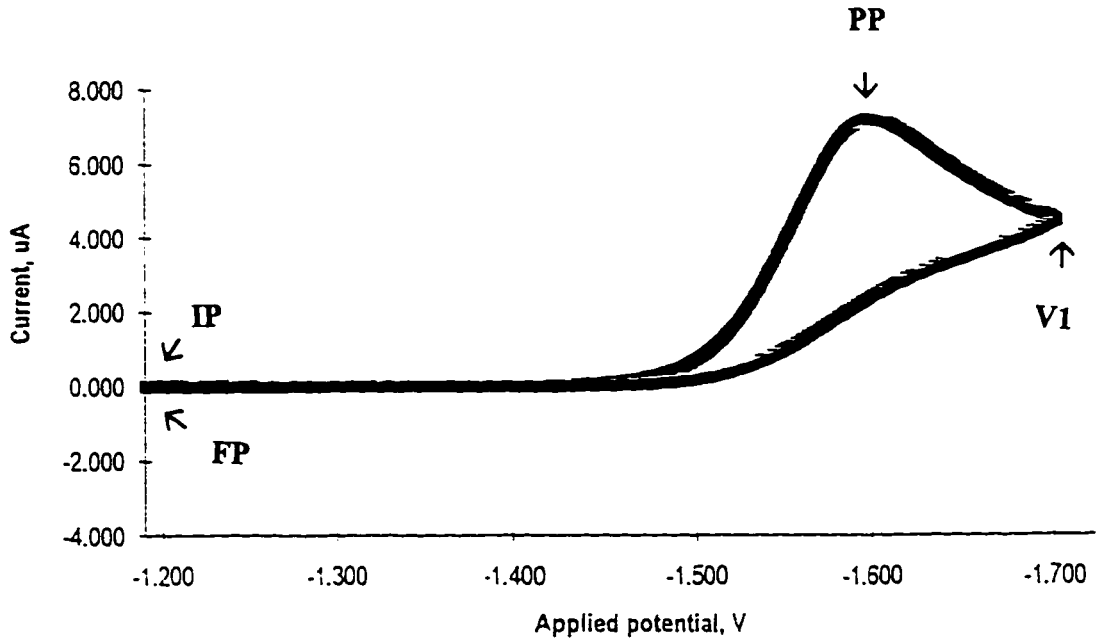

Figure 6. Cyclic voltammogram for an irreversible reaction illustrating: initial potential (IP), peak potential (PP), vertex potential (V1), and final potential (FP).

For this investigation 1024 data points were selected where $2^{10} = 1024$. An initial switching and final potential was used to define a "window" that would collect a total of 1025 data points with the first datum deleted for FFT. The window was positioned in such a way to be large enough to capture all of the meaningful electrochemical information, but to ensure that the primary cathodic peak was located at exactly the same point within the window for each cyclic voltammogram collected. The FFT frequency domain data will only contain fundamental shape information related to different electrochemical behavior and not artifacts due to movement of the peak within the time window.

The experimental procedure began with obtaining an initial cyclic voltammogram to establish the primary cathodic PP. Then, the IP and V1 values were reset such that (V1-PP) was 50 mV or 100 mV. A cyclic voltammogram was rerun with these modified parameters and the voltammogram was examined to confirm that the data window criteria were met.

Equilibration time (ET) refers to the delay time in seconds after a fresh mercury drop has been dispensed. For the purposes of this study this was referred to as hang time. This parameter was set to 1 or 30 seconds.

Acquisition mode (AM) refers to how many times the current is sampled in relation to the step time in the applied voltage waveform. AM choices are: 1/4, 2/4, 3/4, 4/4, All, or Ramp. Fractional modes correspond to which portion of the step time the current is sampled. Using the "All" mode measures at all four intervals, whereas in "Ramp" mode the step is broken into 0.25 mV increments. The 4/4 mode was used for this work because it is has the highest rejection of the charging current background contribution.

Current range (CR) is the maximum current expected for the cyclic voltammogram. For this study CR was set to 10 μA, which was well above the expected maximum current of the cyclic voltammograms that were run. Rise time (RT) defines how quickly the potentiostat is able to respond to a change in potential. RT changes the bandwidth characteristics of the instrument to either one of high stability or high speed. High speed mode was selected because it resulted in better integrity of the data at the switching potential as shown in Figure 7. It can be seen that there is a significant jump observed at the switching potential in the "high stability" mode but not in the "high speed" mode.

A choice of filters was available in the software to reduce the effects of high frequency noise at very low current measurements. Use of a filter is better suited for work with microelectrodes at slow scan rates and was not used in this study.

Scan increment (SI), Scan rate (SR) and Step time (ST) relate to one another by the equation:

$$\text{Scan Rate} = \text{Scan Increment} / \text{Step Time} \qquad (3)$$

Scan rate is set by the analyst and measures how quickly the potential changes in the potential sweep. For this study two rates were used: 250 mV/sec and 1000 mV/sec. Scan increment is a measure between data points in the experiment. It is possible to go to a minimum of 1 mV. In this study either 1 mV or 2 mV was utilized for the one cycle and two cycle experiments respectively. Step time determines how long each scan increment is applied in seconds. For a scan rate of 250 mV/sec with a 1 mV scan increment the resulting step time was 4 milliseconds.

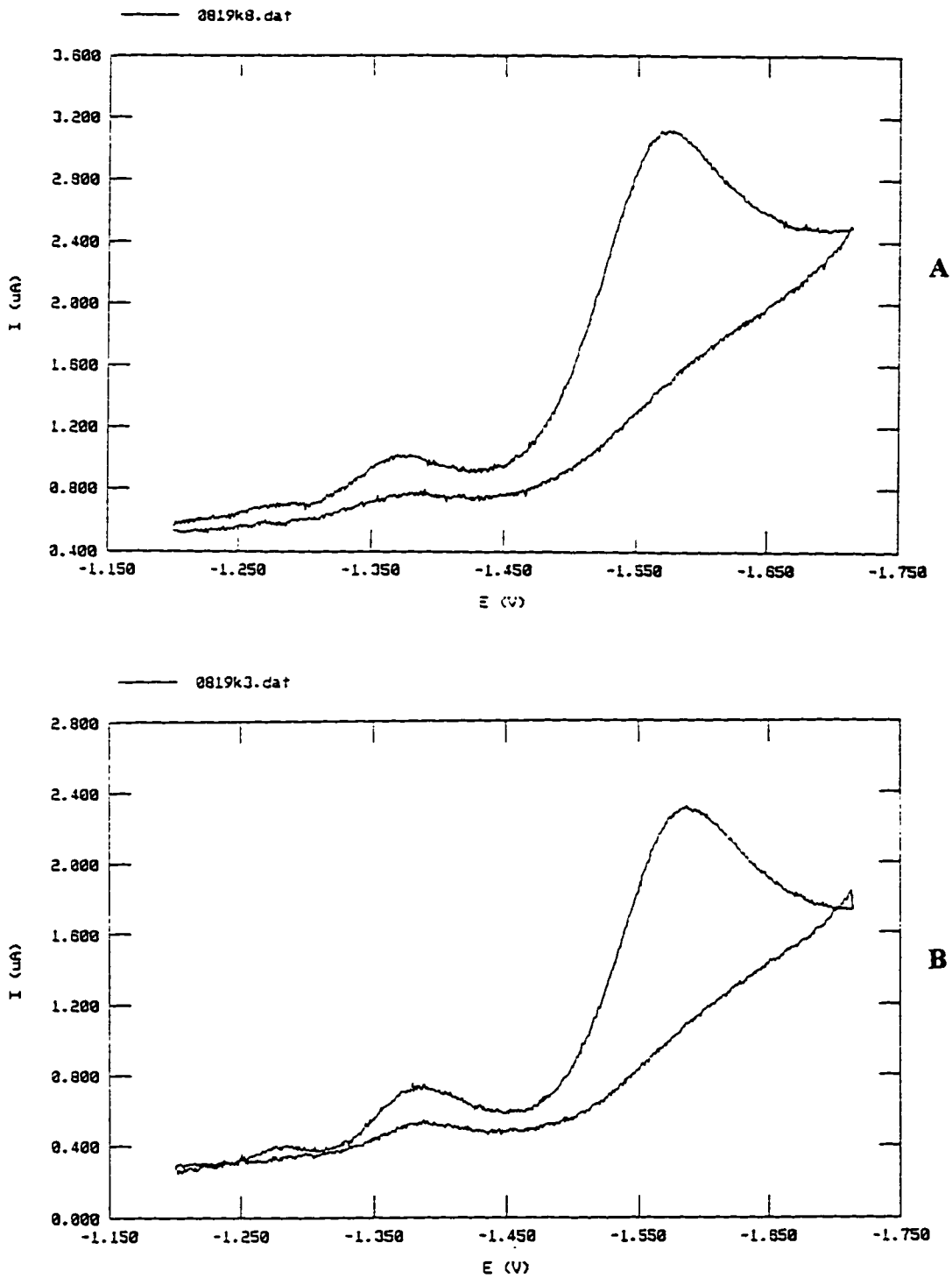

Figure 7. Comparison of high speed (A) and high stability (B) mode for acquiring voltammetric data for experiment 1'. Conditions in Table 3.

The Number of points (NP) is the number of data points collected. It is determined by the potential range and scan increment that was selected. The Number of Cycles (NC) is the number of potential sweep cycles performed. For this study either one or two cycles were performed. A scan rate of either 250 or 1000 mV/sec was used for the cyclic voltammetric (CV) experiments.

C. Voltammetric Response Characteristics

Preliminary voltammetric investigations of aqueous ketorolac solutions revealed the presence of one reduction peak. This is consistent with published studies for the structurally similar analgesic drugs: zomepirac (49) and ketoprofen (50). Figure 8 shows a representative cyclic voltammogram using experiment 7' conditions (see Table 3). A well-defined cathodic peak was observed at -1.576 V. This is understood to be the process for a one-electron reduction of the ketone group based on investigation of 2,6-dichloro-1,4-phenylendiamine by Wandlowski and coworkers (51). No oxidation peak was observed under these conditions for the reverse scan which suggests the presence of a rapid irreversible chemical reaction of the one-electron reduction product.

A blank voltammogram was run to confirm the absence of contamination and to blank-correct voltammograms. A representative voltammetric blank run using experiment 7' conditions is shown in Figure 9. No significant interfering signals were detected in this blank voltammogram.

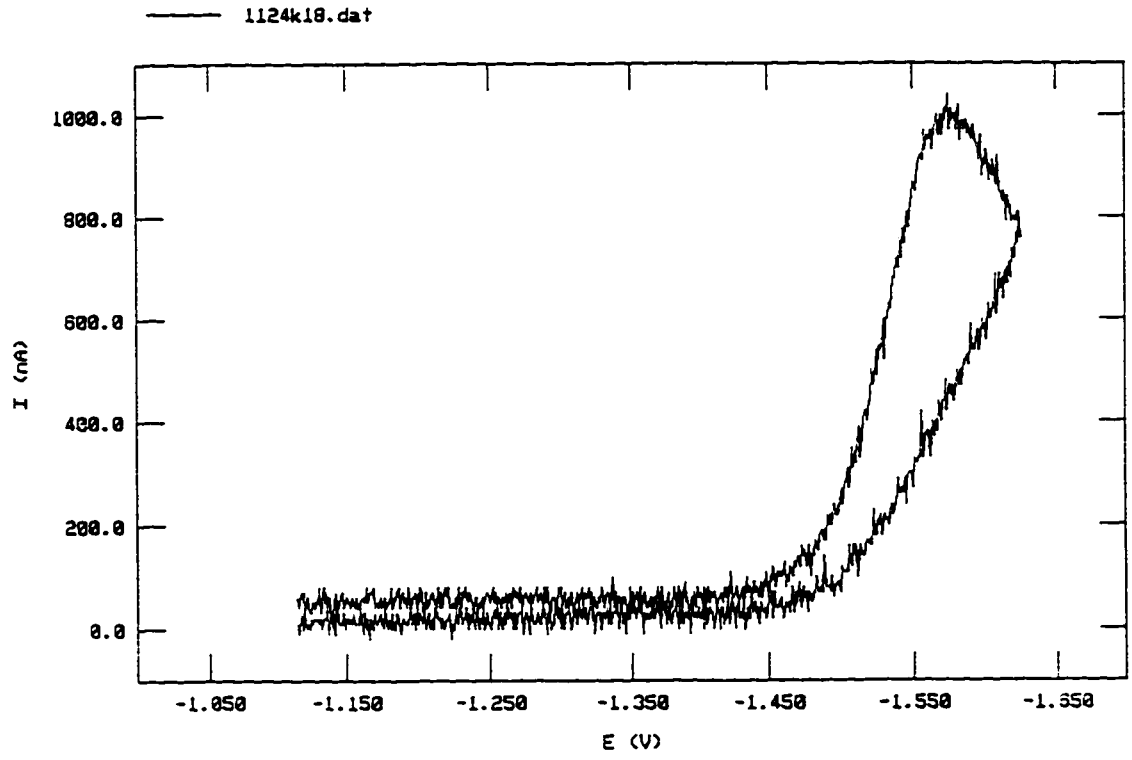

Figure 8. Representative analyte cyclic voltammogram for experiment 7'. Conditions in Table 3.

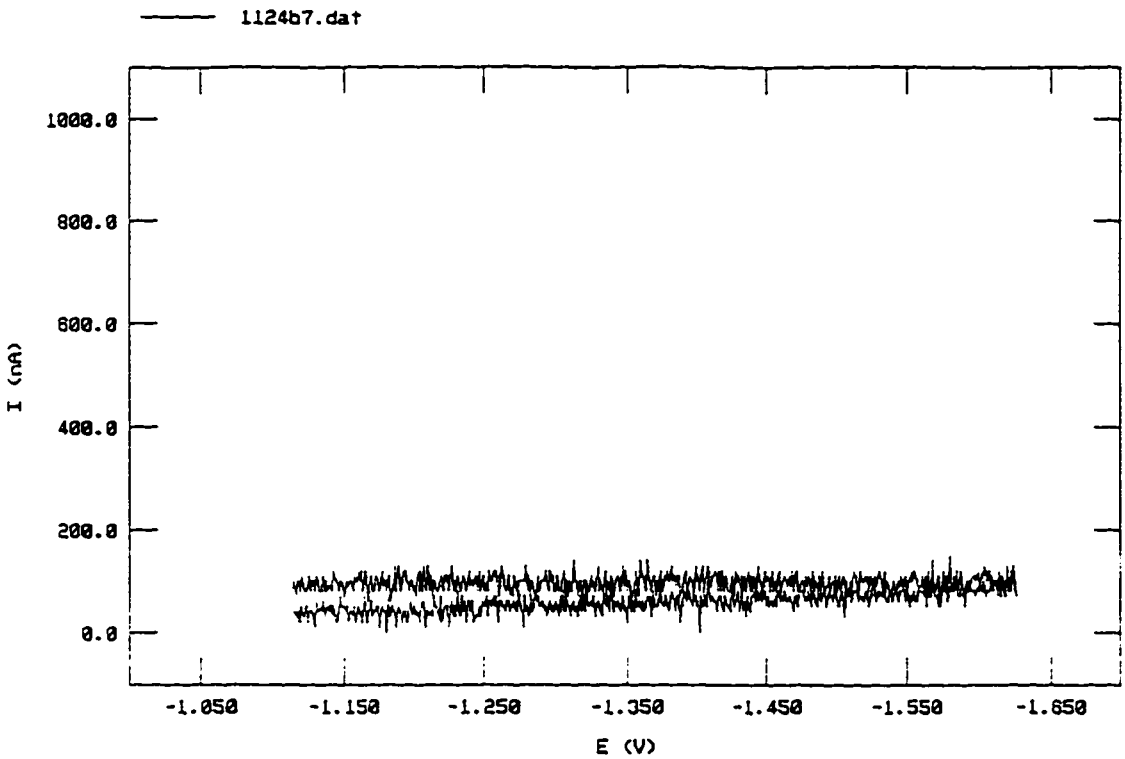

Figure 9. Representative blank cyclic voltammogram using conditions for experiment 7'. Conditions in Table 3.

D. Ensemble Averaging of Voltammetric Data

Nine replicate voltammograms were ensemble averaged to improve signal-to-noise. Each voltammogram was characterized by the starting current, switching current and final current to ensure that each voltammogram was free of extraneous current spikes or other abnormal characteristics. At least fifteen replicate voltammograms were run from which the nine most representative runs were used for ensemble averaging. Figures 10 and 11 illustrate the benefit of ensemble averaging for analyte and blank voltammograms respectively. It can be seen that the noise level was clearly reduced after ensemble averaging.

To quantify the benefit of ensemble averaging, a representative 10 mV portion of the voltammogram was selected. The current readings of the eleven data points from -1.150 to -1.160 V were examined to determine the highest and lowest current reading. The difference between these two values yielded an average peak-to-peak noise reading of 50.00 ± 7.07 nA for the nine blank voltammograms of experiment 7′. For the n=9 ensemble averaged voltammogram, a peak-to-peak noise reading of 16.66 nA was measured. The result of ensemble averaging nine voltammograms was a three-fold reduction in noise.

E. Data Smoothing of Voltammetric Data

Voltammetric signal-to-noise was further enhanced by smoothing the data with a linear (3 point) Savitzky-Golay algorithm. Figures 12 and 13 illustrate the change that occurs when the ensemble averaged voltammogram was smoothed for the blank and analyte voltammograms respectively. The same 10 mV portion of the voltammogram was

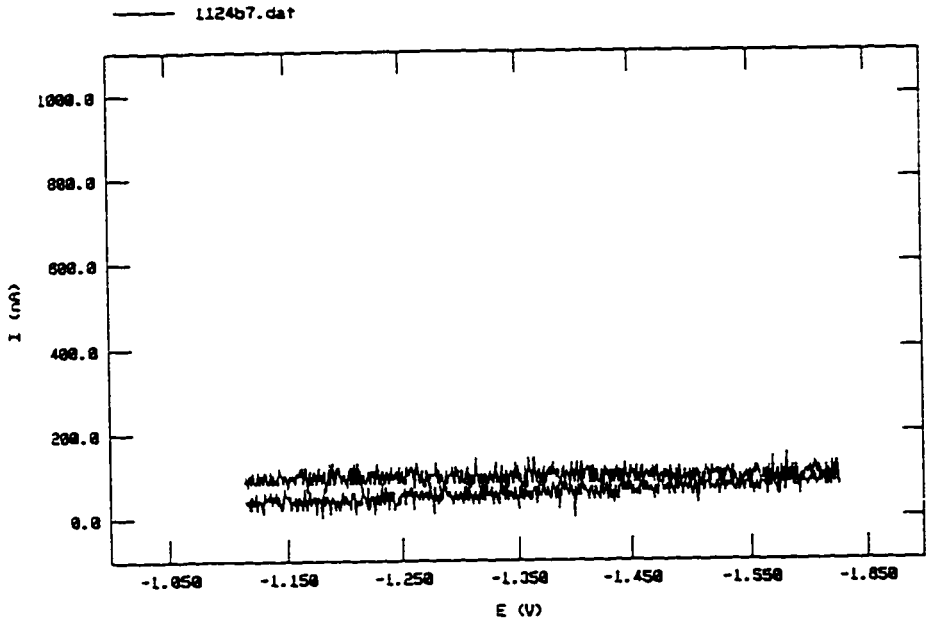

A

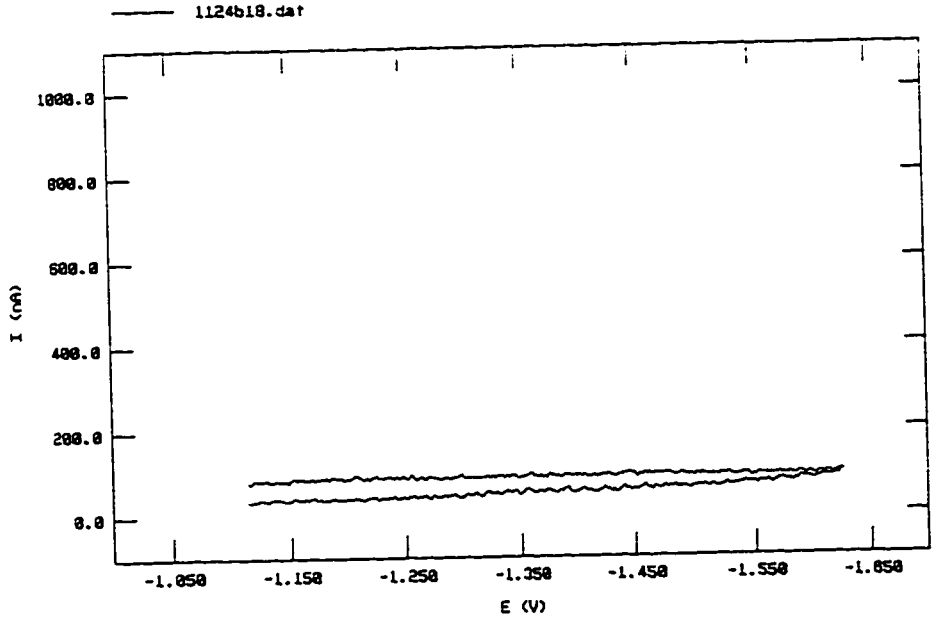

B

Figure 10. Representative blank cyclic voltammogram for experiment 7' single run (A) and ensemble-averaged for n=9 (B). Conditions in Table 3.

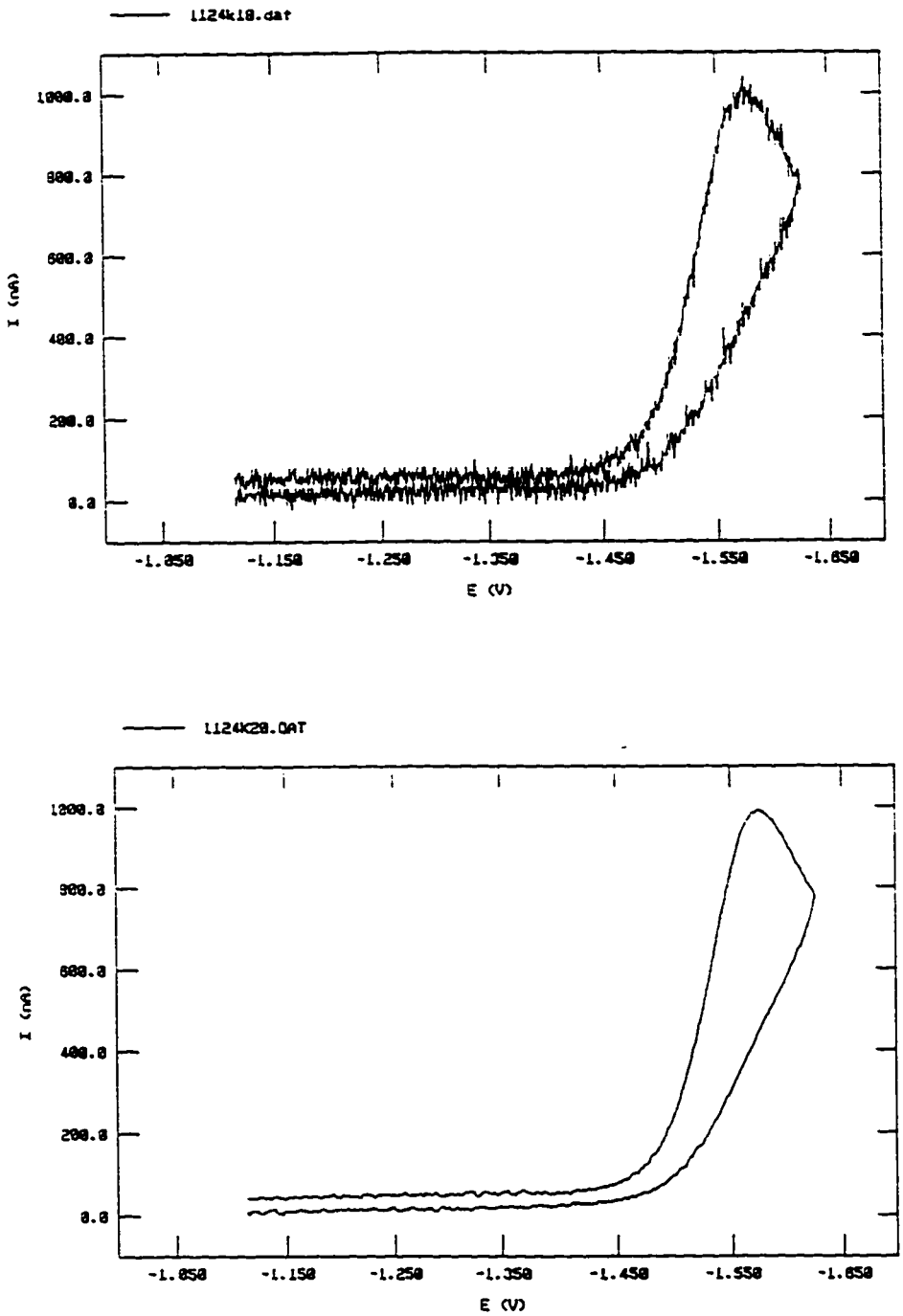

Figure 11. Representative analyte cyclic voltammogram for experiment 7' single run (A) and ensemble-averaged for n=9 (B). Conditions in Table 3.

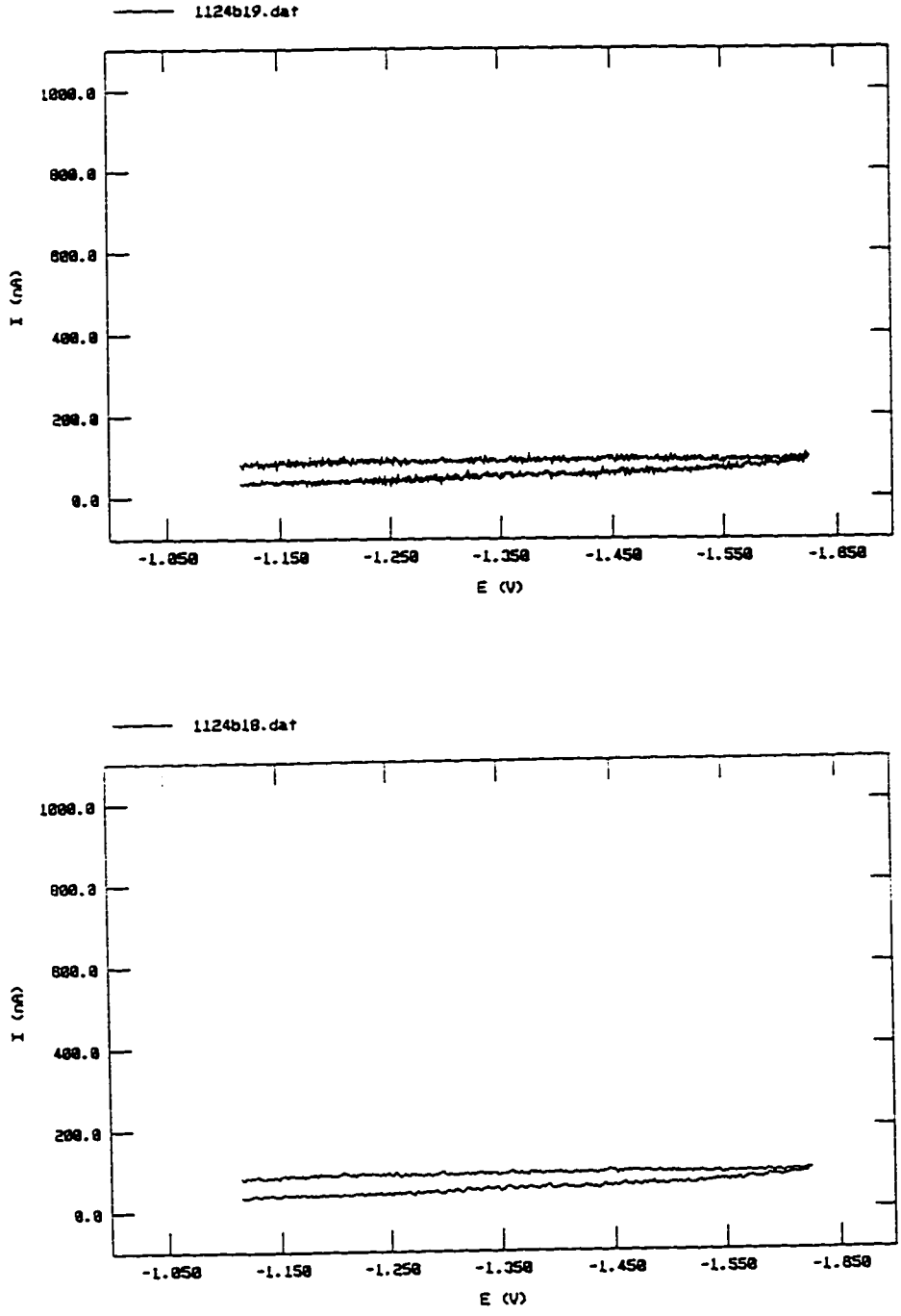

Figure 12. Blank cyclic voltammogram ensemble-averaged for n=9 for experiment 7' without smoothing (A) and with 3 point Savitzky-Golay smoothing (B). Conditions in Table 3.

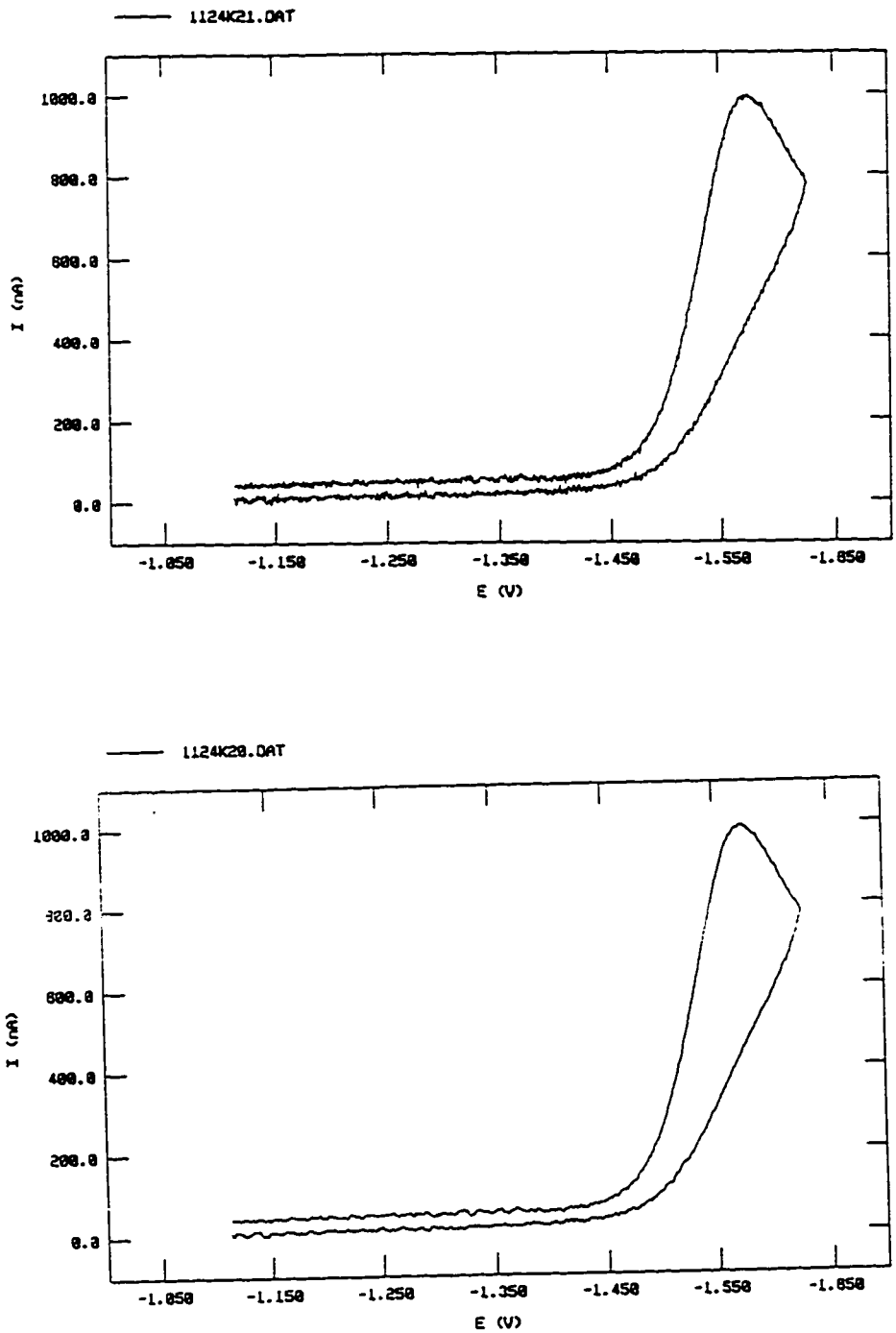

Figure 13. Analyte cyclic voltammogram ensemble-averaged for n=9 for experiment 7' without 3 point Savitzky-Golay smoothing (A) and with 3 point Savitzky-Golay smoothing (B). Conditions in Table 3.

measured for peak-to-peak noise and was found to have been further reduced from 16.66 nA to 5.19 nA. This represents a 10-fold decrease in noise over the original data.

To demonstrate the benefit that both of these techniques have in reducing noise, the same 10mV portion of the voltammogram (-1.150 to -1.160 V) is shown in Figure 14 for the single run, the n=9 ensemble-averaged run and the smoothed ensemble-averaged voltammograms. The reduction in noise is especially beneficial for determining peak current and potential. Figure 15 illustrates the change in a detailed portion of the voltammogram at the cathodic peak for experiment 7′. It was easier to determine peak current and peak potential after the voltammetric data were ensemble averaged and smoothed.

Blank-corrected voltammograms were generated when the smoothed/ensemble averaged blank voltammogram was subtracted point for point from the smoothed/ensemble averaged analytical voltammogram run under the same conditions. Figure 16 shows the blank-corrected voltammogram run for experiment 7′. It can be seen that the subtraction of the blank shifted the baseline to zero current at the potential where no redox processes occurred.

F. Voltammetric Results

The final ensemble-averaged, smoothed and blank-corrected voltammograms for the sequence of twelve experiments are shown in Figures 17 - 22. It can be seen that a variation in current response, number of cathodic peaks, and noise level was obtained for these runs. Of interest is the number of cathodic peaks. Two cathodic peaks were observed for experiments 1′ - 4′ run at pH 7 and experiments 5′′ - 8′′ run at pH 6.

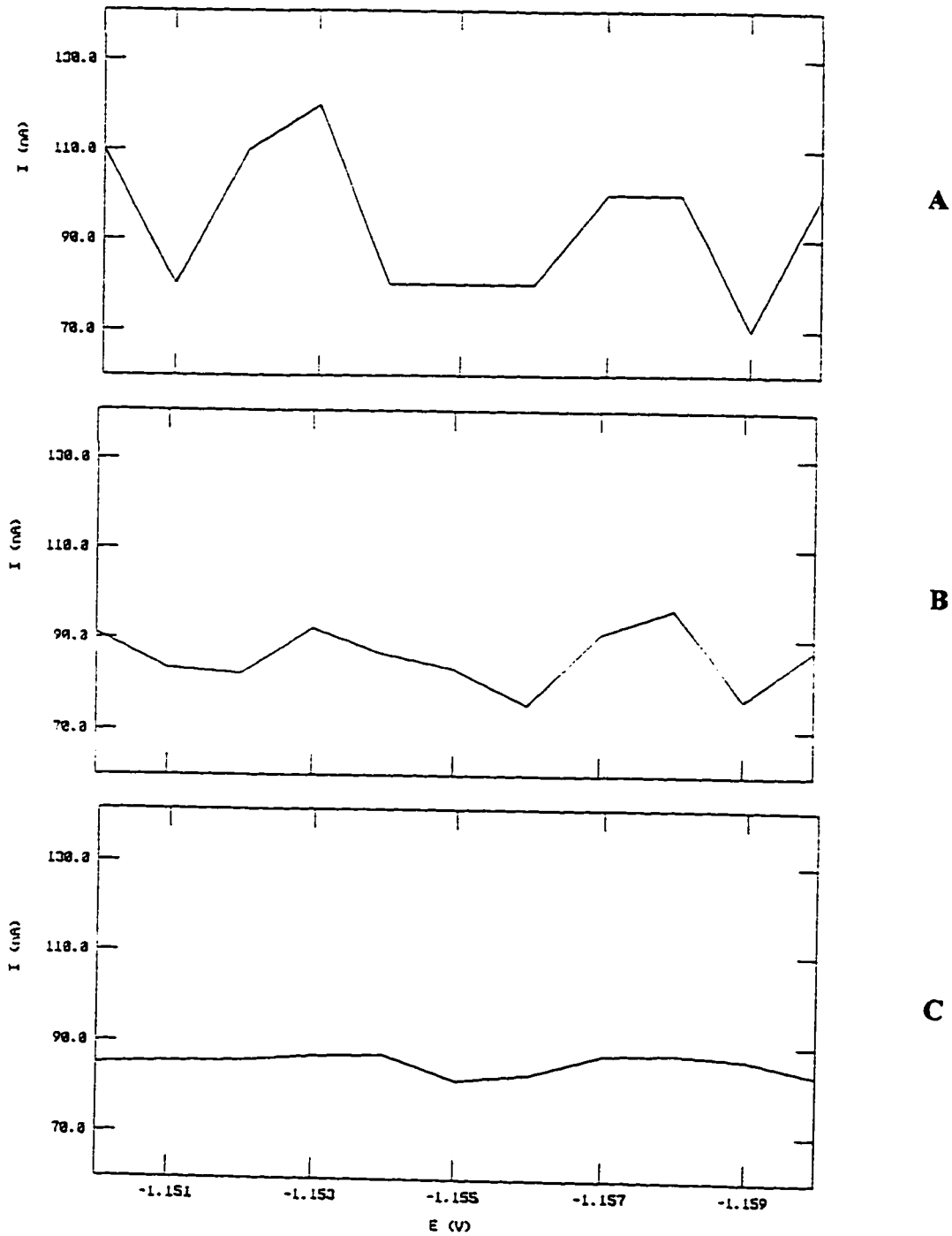

Figure 14. Detail of blank cyclic voltammogram for experiment 7' for single run (A), ensemble-averaged for n=9 (B), and ensemble-averaged for n=9 with 3 point Savitzky-Golay smoothing (C). Conditions in Table 3.

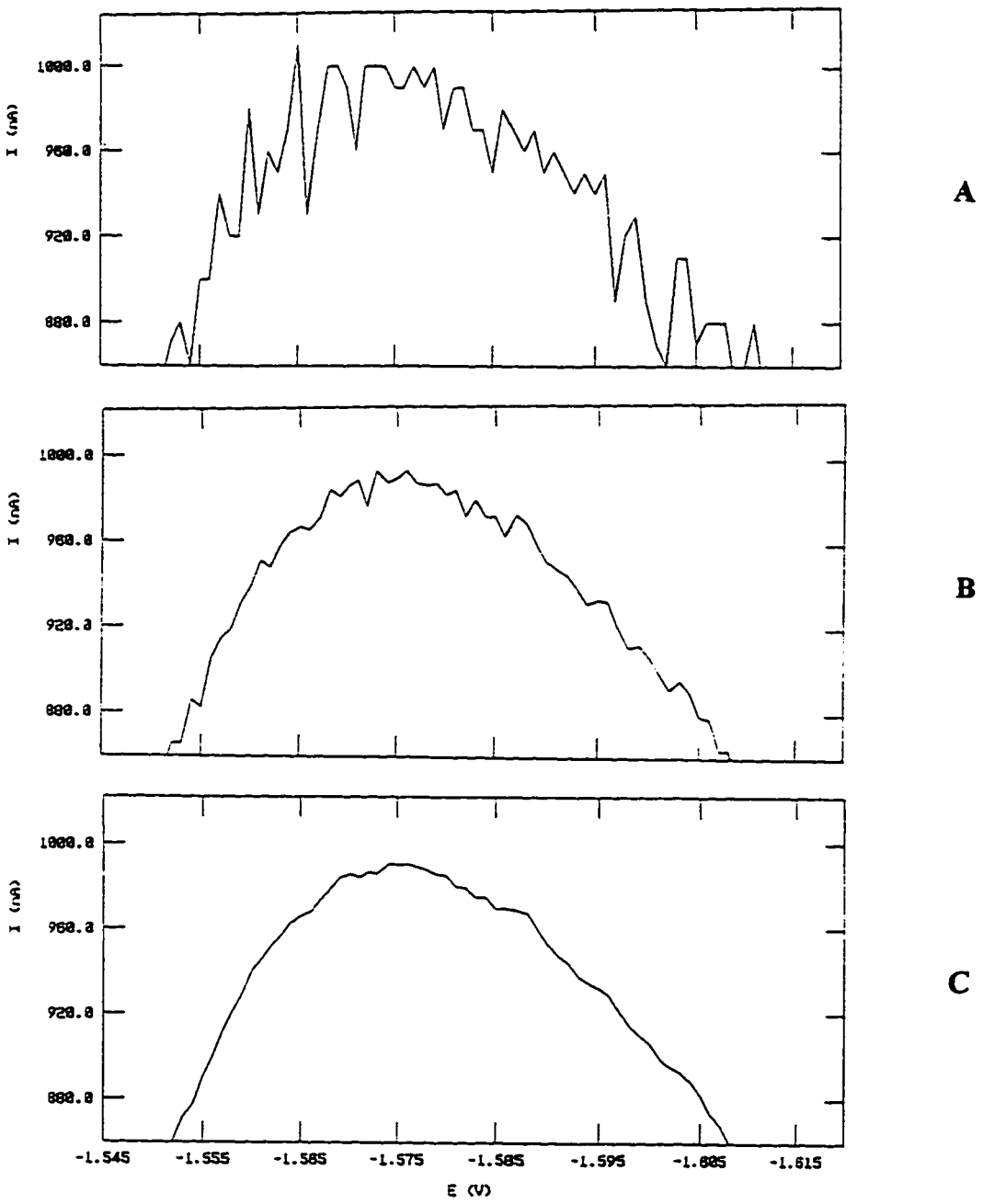

Figure 15. Detail of analyte cyclic voltammogram using conditions for experiment 7' for single run (A), ensemble-averaged for n=9 (B), and ensemble-averaged for n=9 with 3 point Savitzky-Golay smoothing (C). Conditions in Table 3.

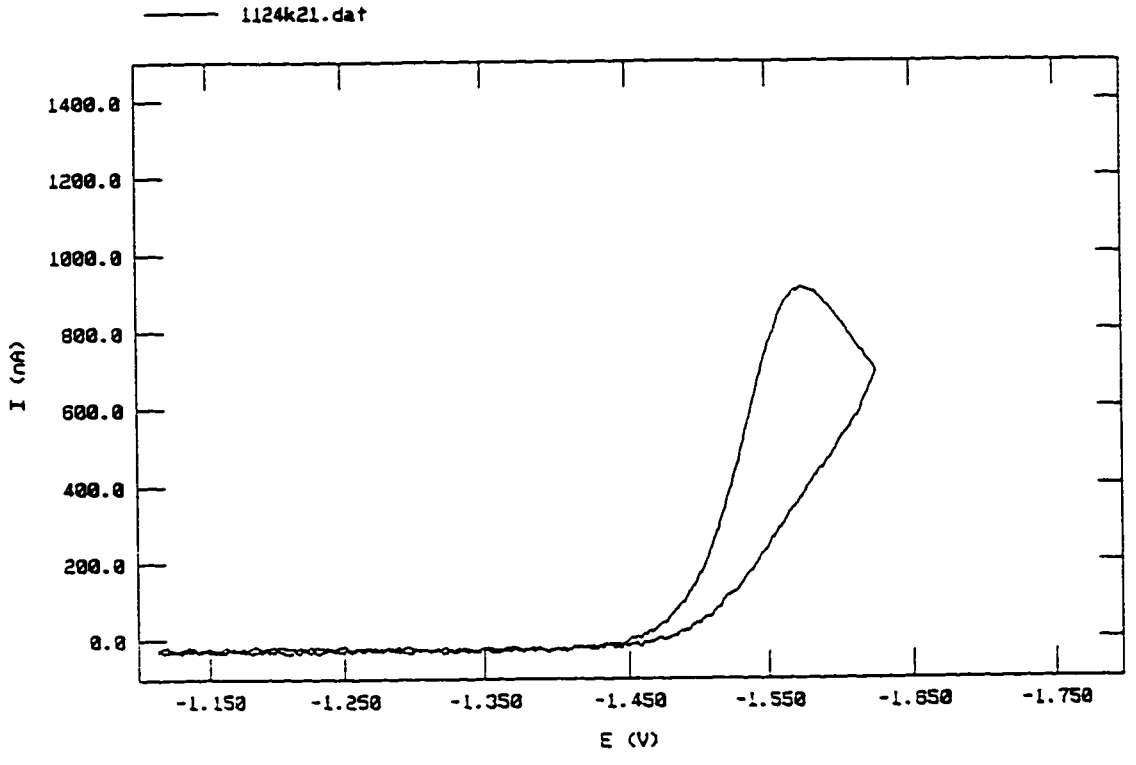

Figure 16. Ensemble-averaged, smoothed and blank corrected analyte cyclic voltammogram for experiment 7'. Conditions in Table 3.

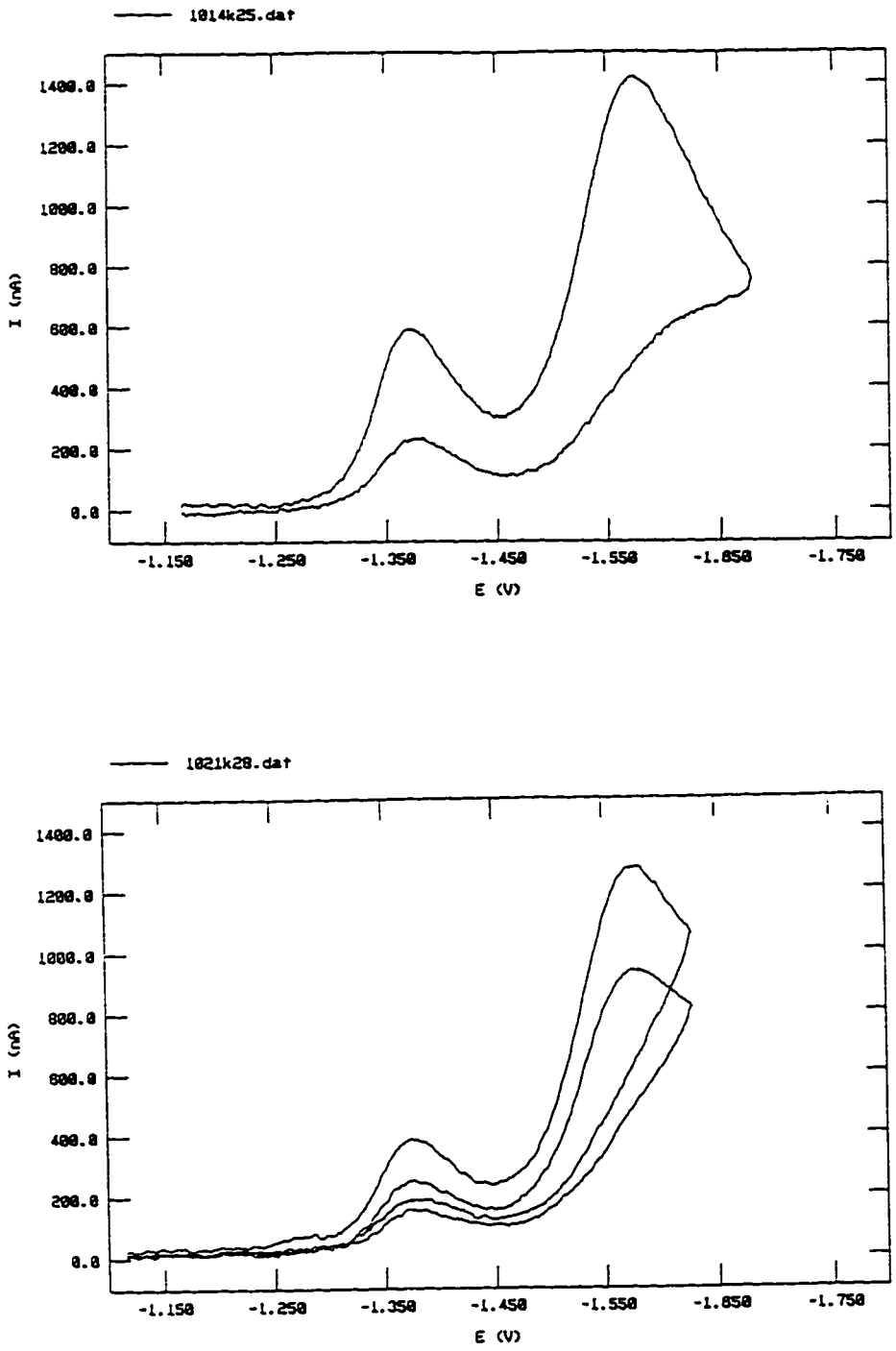

Figure 17. Ensemble-averaged, smoothed and blank corrected analyte cyclic voltammograms for experiment 1' (A) and experiment 2' (B). Conditions in Table 3.

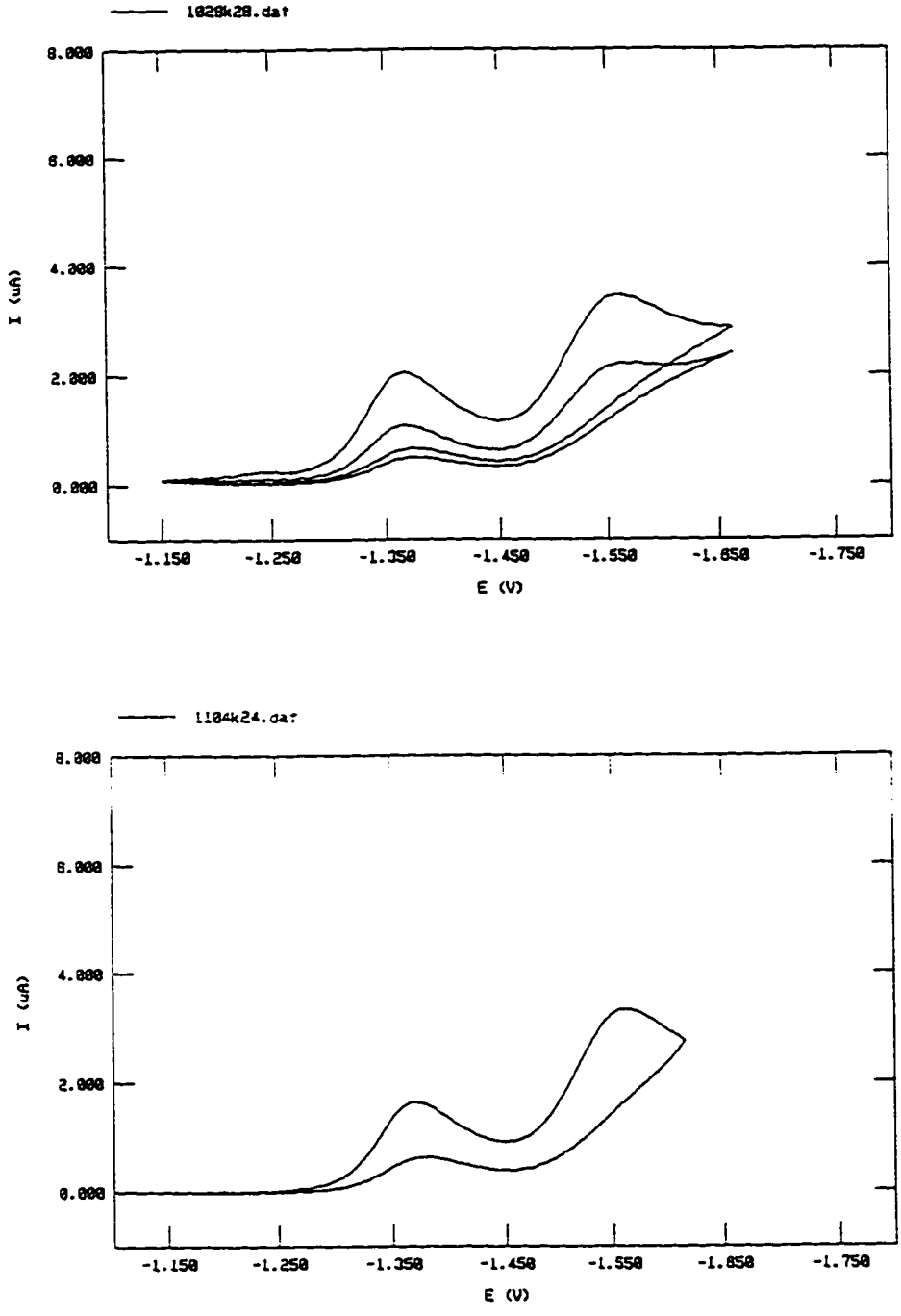

Figure 18. Ensemble-averaged, smoothed and blank corrected analyte cyclic voltammograms for experiment 3' (A) and experiment 4' (B). Conditions in Table 3.

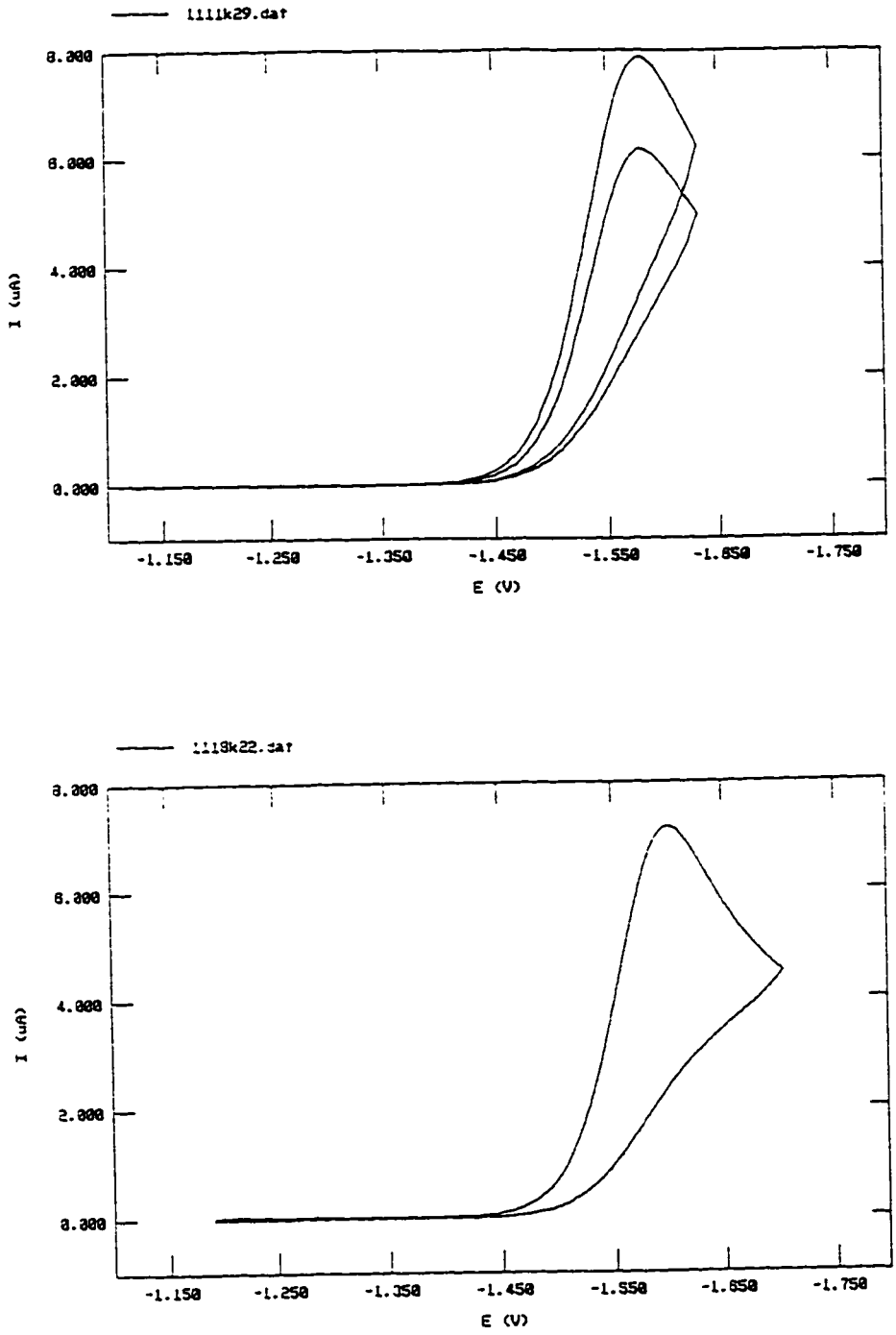

Figure 19. Ensemble-averaged, smoothed and blank corrected analyte cyclic voltammograms: experiment 5' (A) and experiment 6' (B). Conditions in Table 3.

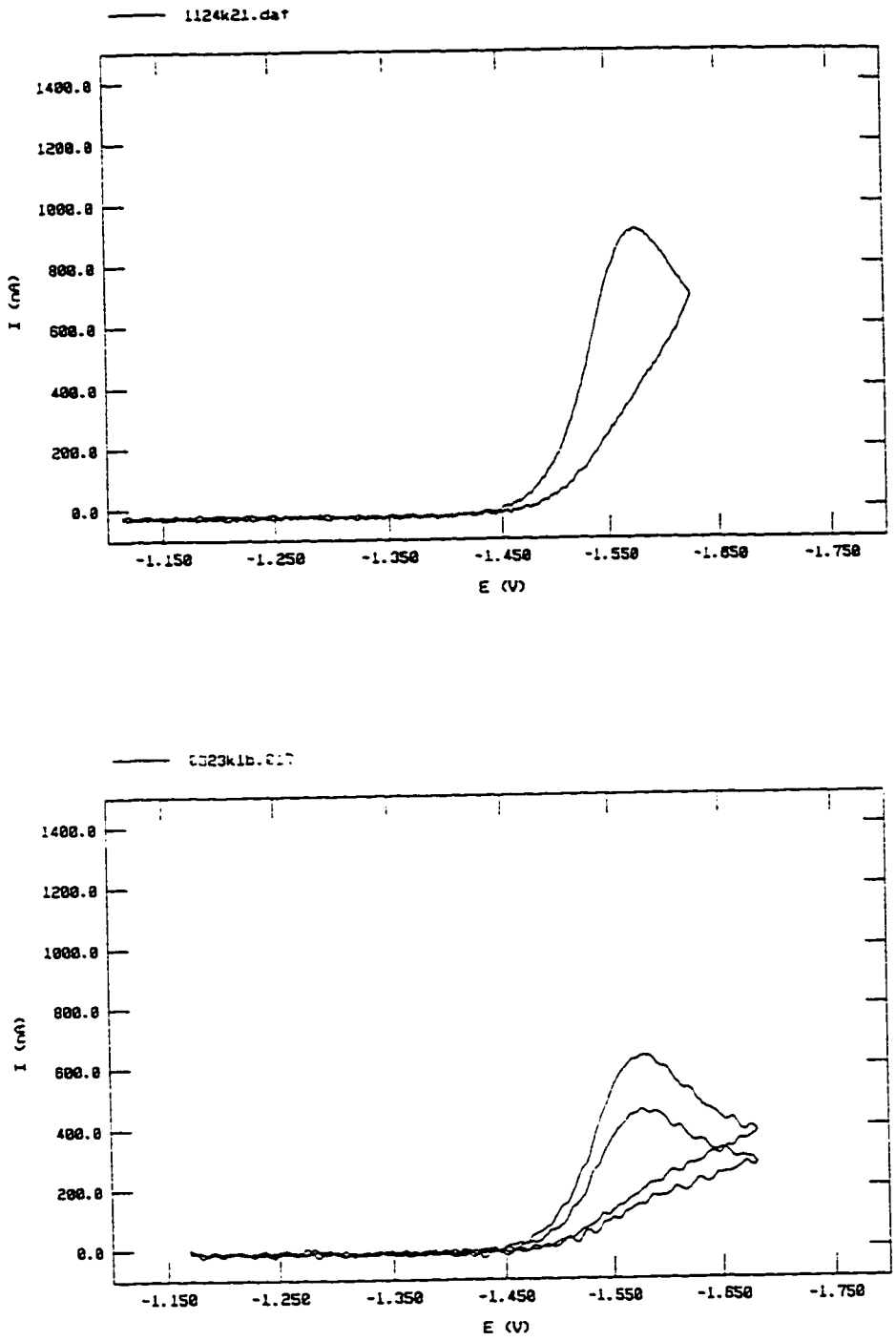

Figure 20. Ensemble-averaged, smoothed and blank corrected analyte cyclic voltammograms: experiment 7' (A) and experiment 8' (B). Conditions in Table 3.

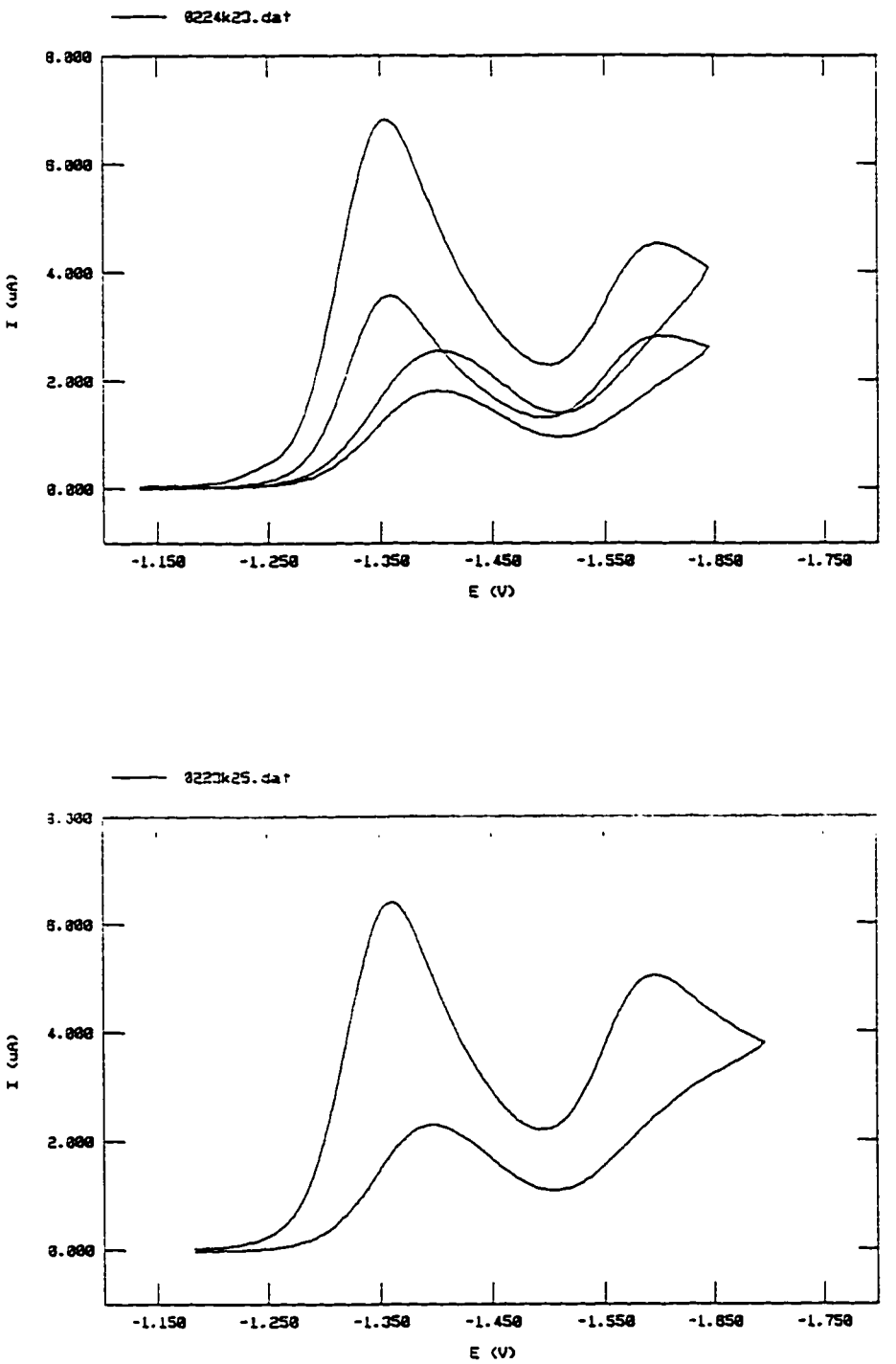

Figure 21. Ensemble-averaged, smoothed and blank corrected analyte cyclic voltammograms: experiment 5" (A) and experiment 6" (B). Conditions in Table 3.

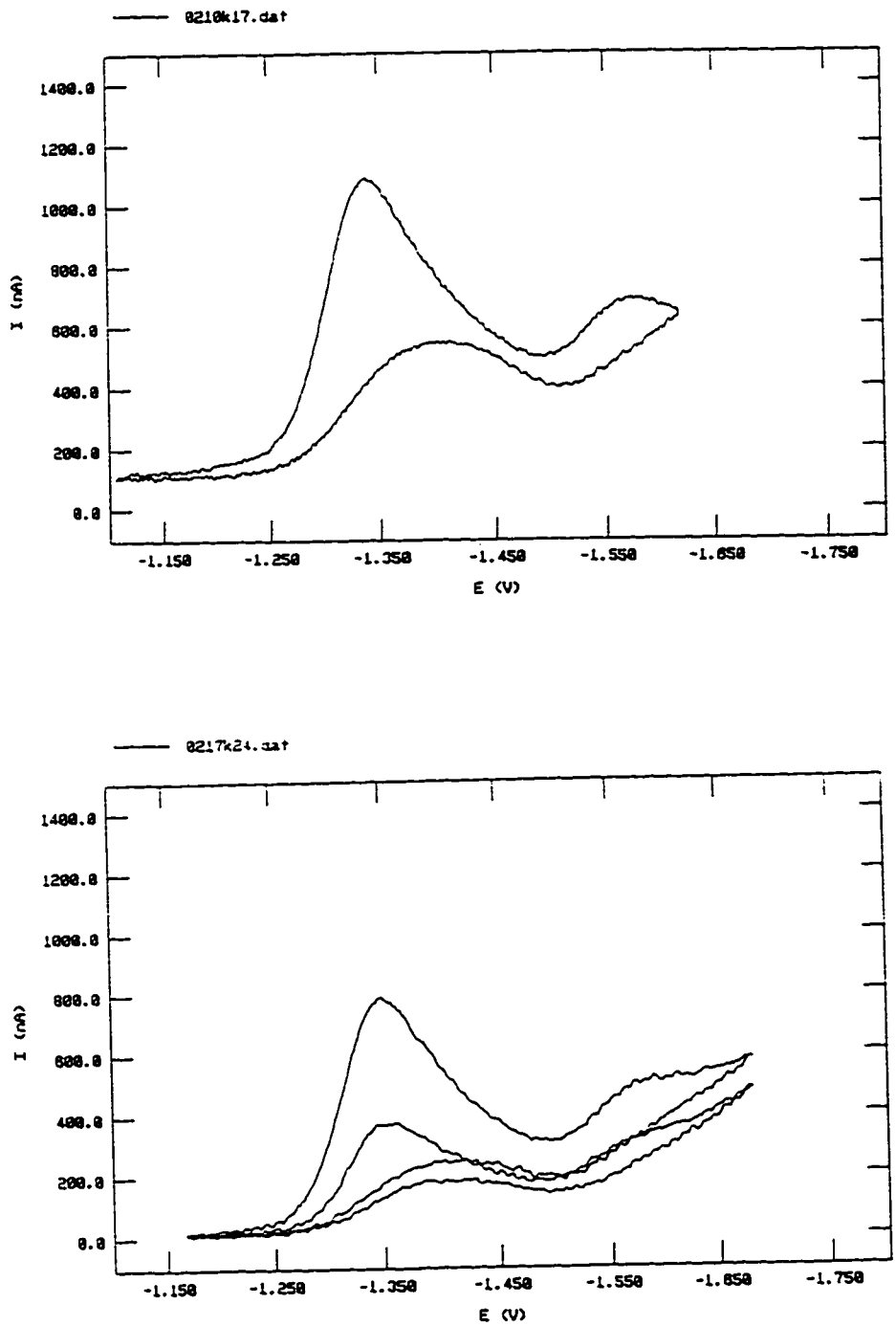

Figure 22. Ensemble-averaged, smoothed and blank corrected analyte cyclic voltammograms: experiment 7" (A) and experiment 8" (B). Conditions in Table 3.

Whereas for experiments 5′ - 8′ run at pH 11 only one cathodic was observed. For identification purposes, the cathodic peak at the less negative potential was labeled "A" (~ -1.4 V), the cathodic peak at the more negative potential was labeled "B" (~ -1.6 V), and the cathodic peak observed in the anodic scan is labeled "A′ " as illustrated in Figure 23. A summary of the peak potentials, as well as the initial and vertex (or switching) potentials for the twelve experiments is listed in Table 7. In cases where multiple scans were run only the first scan was considered.

In the case of the voltammograms for experiments 1′ through 4′ run at pH 7, two cathodic peaks were observed. To calculate the peak current for peak B, the decaying current of the peak A was used as the baseline. This was done by assuming that the current decays with a $1/(t^{½})$ dependence. The voltammetric data for experiments with two cathodic peaks was processed using the voltammetric processing procedure described by Perone and coworkers (52). The following equation was utilized to calculate the current decay

$$i_{(t+to)} = i_o[t_o/(t + t_o)]^{½} \qquad (4)$$

where i_o is the current at t_o and t is the time past t_o.

To process the voltammograms, the digital data were imported from the electrochemical software into a spreadsheet program and processed with eq 4. The data in Table 8 illustrate how this was accomplished for experiment 1′. The data points shown are from the receding portion of the previous voltammetric peak A after the peak is selected to represent t_o, and the measured current values were processed to give a fit to eq 4 with less than 1% deviation. This curve was then extended past the peak potential of peak B

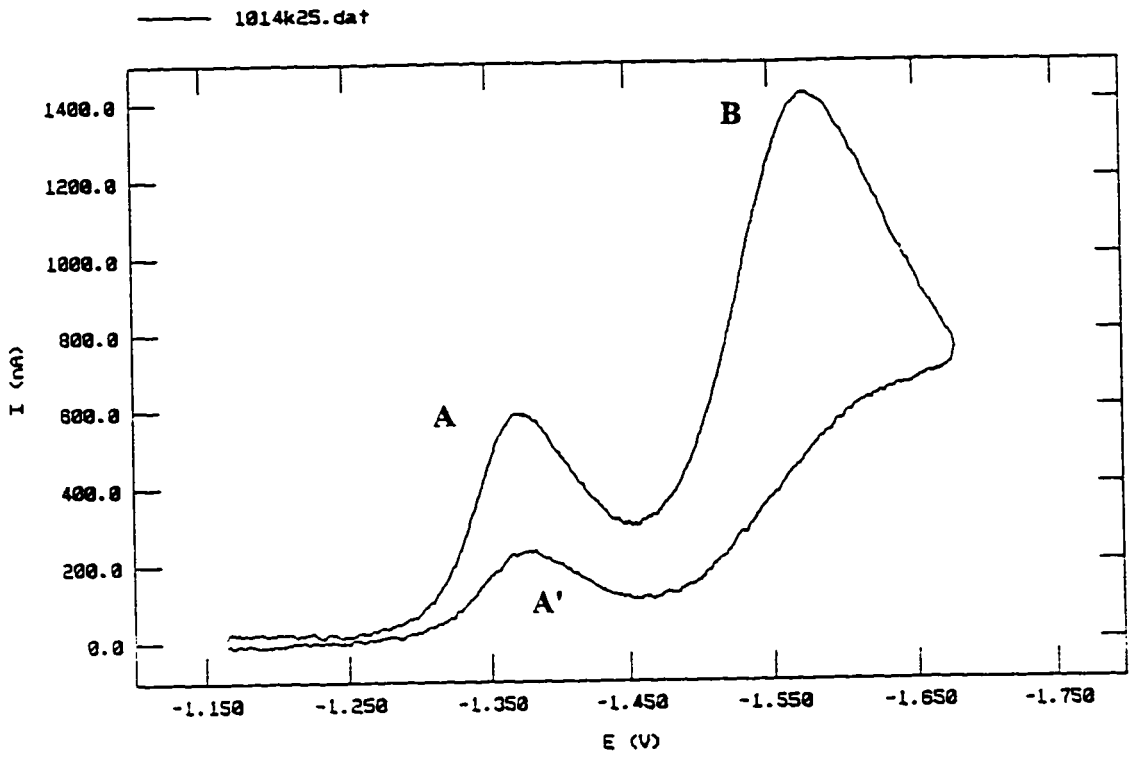

Figure 23. Ensemble-averaged, smoothed and blank-corrected analyte cyclic voltammograms for experiment 1' illustrating cathodic peak A, cathodic peak B, and reduction peak on anodic sweep A'. Conditions in Table 3.

Table 7. Experimental Design Voltammetric Results

Experiment number	Initial potential (IP), V	Peak A potential (PP), V	Peak B potential (PP), V	Vertex 1 potential (V1), V
1'	-1.165	-1.375	-1.576	-1.677
2'	-1.116	-1.376	-1.578	-1.628
3'	-1.150	-1.368	-1.562	-1.662
4'	-1.103	-1.372	-1.564	-1.615
5'	-1.120	-	-1.580	-1.632
6'	-1.190	-	-1.601	-1.702
7'	-1.113	-	-1.576	-1.625
8'	-1.170	-	-1.582	-1.682
5''	-1.133	-1.353	-1.596	-1.645
6''	-1.184	-1.360	-1.596	-1.696
7''	-1.106	-1.338	-1.580	-1.618
8''	-1.168	-1.350	-1.580	-1.680

Table 8. Diffusion-Controlled Baseline Processing for Experiment 1'

Data point #	Time sec $(t - t_o)$	Applied potential V	Actual Current μA	Peak A Calculated Current μA	100 - Calc. Cur. / Act. * 100 %	Remarks
210	0.210	-1.374	0.587	-	-	
211	0.211	-1.375	0.583	-	-	Peak A
212	0.212	-1.376	0.587	-	-	
225	0.225	-1.389	0.547	0.547	-	
226	0.226	-1.390	0.539	0.541	0.3	
227	0.227	-1.391	0.536	0.535	-0.1	
228	0.228	-1.392	0.529	0.530	0.1	
229	0.229	-1.393	0.523	0.524	0.1	
230	0.230	-1.394	0.516	0.518	0.5	
231	0.231	-1.395	0.510	0.513	0.6	
232	0.232	-1.396	0.503	0.507	0.9	
233	0.233	-1.397	0.495	0.502	1.3	
234	0.234	-1.398	0.493	0.496	0.6	
235	0.235	-1.399	0.488	0.491	0.7	
236	0.236	-1.400	0.489	0.486	-0.6	
237	0.237	-1.401	0.478	0.481	0.6	
238	0.238	-1.402	0.474	0.475	0.2	
239	0.239	-1.403	0.470	0.470	0.9	
240	0.240	-1.404	0.464	0.465	0.2	
241	0.241	-1.405	0.457	0.460	0.6	
242	0.242	-1.406	0.456	0.455	-0.1	
243	0.243	-1.407	0.445	0.451	1.2	
244	0.244	-1.408	0.445	0.446	0.2	
245	0.245	-1.409	0.437	0.441	0.9	
246	0.246	-1.410	0.434	0.436	0.5	
Avg.					0.5	226-246
411	0.411	-1.575	1.416	0.074	-	
412	0.412	-1.576	1.415	0.073	-	Peak B
413	0.413	-1.577	1.413	0.072	-	
436	0.436	-1.600	1.313	0.056	-	End

from which a corrected peak current and peak potential values were calculated. The corrected value of PP was used to reset IP and P1 to collect the cyclic voltammogram within the proper window for subsequent FFT. Figure 24 shows the result of processing the voltammogram for experiment 1′. Comparable results were obtained when processing the other seven voltammograms with two cathodic peaks. A summary for the diffusion-controlled baseline processing of peak B in experiment 1′ - 4′ and 5′′ - 8′′ voltammograms is shown in Table 9. In cases where multiple scans were run, only the first scan was considered.

G. Evaluation of Variable Effects

To characterize these voltammetric data the following figures of merit were determined: cathodic peak potential and cathodic peak current. (The absence of an anodic peak in the voltammograms did not permit the use of this figure of merit as well as criteria based on the ratio of peak currents.) With the use of cathodic peak potentials as well as the analyte concentration and the scan rate it was possible to calculate a figure of merit for the twelve experiments. The Randles-Sevcik equation (53) was used for this purpose

$$i_p = 269\, n^{3/2} A D^{1/2} v^{1/2} C^b \qquad (5)$$

where i_p = peak height (amps)

n = number of electrons

A = area (cm^2)

D = diffusion coefficient ($cm^2\ sec^{-1}$)

v = scan rate (volts sec^{-1})

C^b =concentration in the bulk of solution (molar)

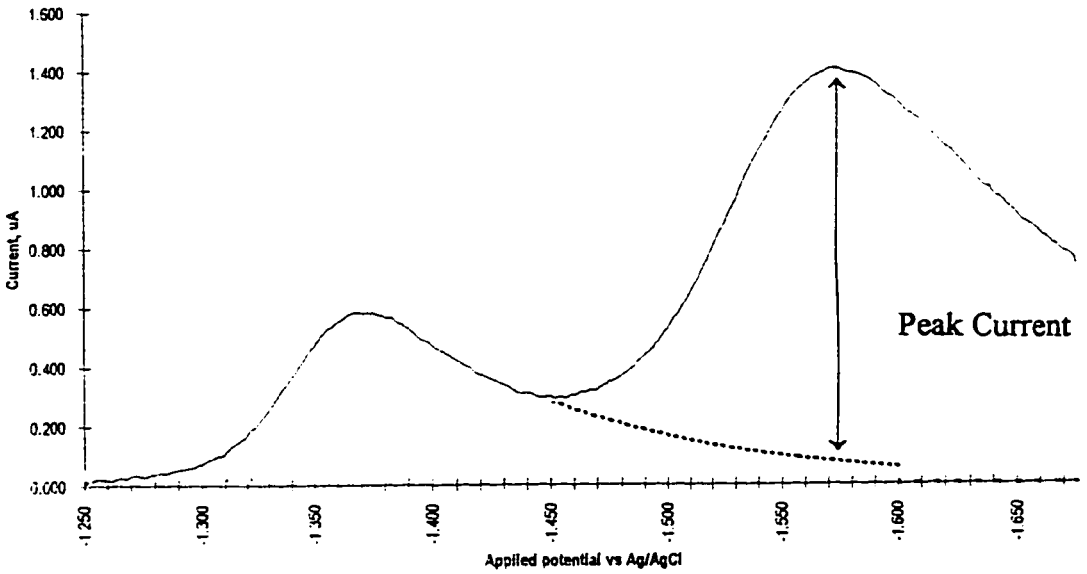

Figure 24. Detail of experiment 1' blank-corrected analyte cyclic voltammogram processed to define diffusion-controlled baseline region (dotted line) for peak B. Conditions in Table 3.

Table 9. Diffusion-Controlled Baseline Processing Results

Experiment number	i_p Peak A Current	i_p Peak B Current	Estimated Diffusion Current Baseline	i_p Corrected Peak B Current
	μA	μA	μA	μA
1′	0.583	1.415	0.073	1.342
2′	0.383	1.271	0.072	1.199
3′	2.054	3.463	0.237	3.226
4′	1.632	3.584	0.363	3.221
5′	-	7.866	-	-
6′	-	7.170	-	-
7′	-	0.990	-	-
8′	-	0.629	-	-
5″	6.810	4.516	0.838	3.678
6″	6.408	5.044	0.756	4.288
7″	0.987	0.500	0.395	0.105
8″	0.790	0.581	0.133	0.448

Constants in the equation which include the number of electrons, area of the electrode, and the diffusion coefficient can be condensed into a single factor, **K**. Thus eq 5 becomes

$$i_p = \mathbf{K}\, v^{1/2}\, C^b \qquad (6)$$

Rearranging eq 6 yielded an equation to calculate the current function, **K** which can be used as a figure of merit to evaluate the results of the twelve voltammetric experiments

$$\mathbf{K} = i_p / (v^{1/2}\, C^b) \qquad (7)$$

A summary of the calculated values for **K** using cathodic peak A and B currents are given in Table 10. In cases where multiple scans were run only the first scan was considered.

The seven factors (pH, analyte concentration, methanol concentration, scan rate, number of cycles, switching potential and hang time) were examined using the calculated values for $i_p / (v^{1/2}\, C^b)$. The effect of a particular variable was calculated using

$$E_x = \Sigma\, \mathbf{K}(+)\, /4 - \Sigma\, \mathbf{K}(-)\, /4 \qquad (8)$$

where E_x is the effect of particular factor, **K**(+) is the total response at the high level and **K**(-) is the total response at the low level (54). Table 11 illustrates how the peak B factor effect for scan rate using $i_p / (v^{1/2}\, C^b)$ was calculated. In the same manner the factor effects were calculated for the other factors. The last two factors (number of cycles and switching potential) are dummy variables and were used to measure variability of the system.

The results of the factor effect calculations for cathodic peak B at pH 7 and 11, cathodic peak B at pH 6 and 7, and cathodic peak A at pH 6 and 7, are summarized in Tables 12 -14 respectively. A series of bar charts displays the values of these tables in Figures 25 - 27. It is possible to make several observations upon review of the bar charts.

Table 10. Calculated Current Function [$i_p/ (v^{1/2} C^b)$], for Cathodic Peaks A and B Voltammetric Data

	Peak A	**Peak B**
Experiment number	**$i_p/ (v^{1/2} C^b)$**	**$i_p/ (v^{1/2} C^b)$**
1'	184.4	424.4
2'	121.1	379.2
3'	65.0	102.0
4'	51.6	101.9
5'	-	497.5
6'	-	453.5
7'	-	156.5
8'	-	99.5
5''	430.7	232.6
6''	405.3	271.2
7''	156.1	16.6
8''	124.9	70.8

Table 11. Calculating the Effect of Scan Rate on Peak B Using Current Function $[i_p/ (v^{1/2} C^b)]$

Description		1000 mV/sec K (+)	250 mV/sec K (-)
Experiment	1'	424.4	-
	2'	379.2	-
	3'	-	102.0
	4'	-	101.9
	5'	497.5	-
	6'	453.5	-
	7'	-	156.5
	8'	-	99.5
Sum		1754.5	459.9
Sum /4		438.7	115.0
Δ Sum /4		323.7	

Table 12. Summary of Factor Effects on Current Function [$i_p/ (v^{1/2} C^b)$] from Peak B Voltammetric Data at pH 7 and 11 Using Voltammetric Data for Experiments 1' - 8'

Factor	**K (+)**	**K (-)**	**Factor Effect**
	Sum /4	**Sum /4**	**Δ Sum /4**
pH	251.9	301.8	-49.9
Analyte Concentration	288.7	264.9	23.8
Methanol Concentration	258.5	295.1	-36.6
Scan Rate	438.7	115.0	323.7
Hang Time	280.8	272.8	8.0
Number of cycles *	269.6	284.1	-14.5
Switching potential *	269.9	283.8	-13.9

* = Dummy variables

Table 13. Summary of Factor Effects on Current Function [i_p/ ($v^{1/2}$ C^b)] for Peak B Voltammetric Data at pH 6 and 7 Using Voltammetric Data from Experiments 1' - 4' and 5'' - 8''.

Factor	**R(+)**	**R(-)**	**Factor Effect**
	Sum /4	**Sum /4**	**Δ Sum /4**
pH	147.8	251.9	-104.1
Analyte Concentration	176.9	222.8	- 45.8
Methanol Concentration	205.8	193.9	11.9
Scan Rate	326.9	72.8	254.0
Hang Time	207.4	192.3	15.2
Number of cycles *	262.4	249.1	13.3
Switching potential *	262.7	248.8	13.9

* = Dummy variables

Table 14. Summary of Factor Effects on Current Function [$i_p/ (v^{1/2} C^b)$] for Peak A Voltammetric Data at pH 6 and 7 Using Voltammetric Data from Experiments 1' - 4' and 5'' - 8''.

Factor	**R(+)**	**R(-)**	**Factor Effects**
	Sum /4	**Sum /4**	**Δ Sum /4**
pH	105.5	279.3	-173.7
Analyte Concentration	238.2	146.6	91.5
Methanol Concentration	175.7	209.1	- 33.3
Scan Rate	285.4	99.4	186.0
Hang Time	197.9	186.9	11.0
Number of cycles *	185.4	199.4	- 13.9
Switching potential *	194.9	189.9	5.0

* = Dummy variables

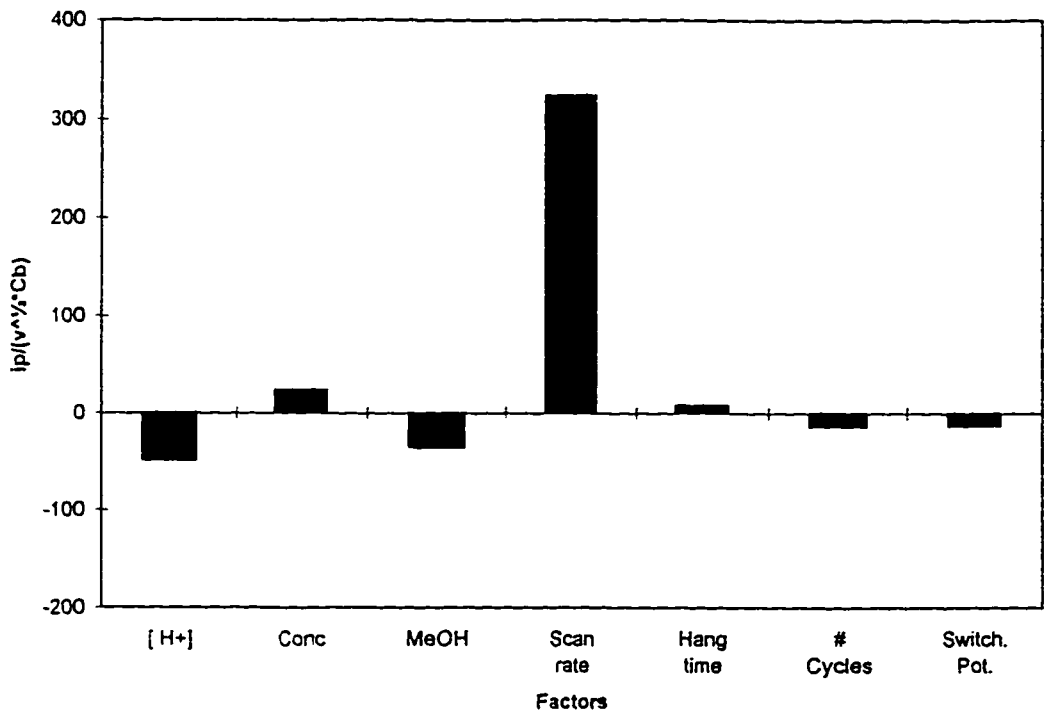

Figure 25. Calculated factor effect on the current function $i_p/ (v^{½} C^{b})$ for peak B at pH 11 and pH 7 for the seven factors: pH, analyte concentration, methanol concentration, scan rate, hang time, number of cycles, and switching potential using experiments 1' - 8'.

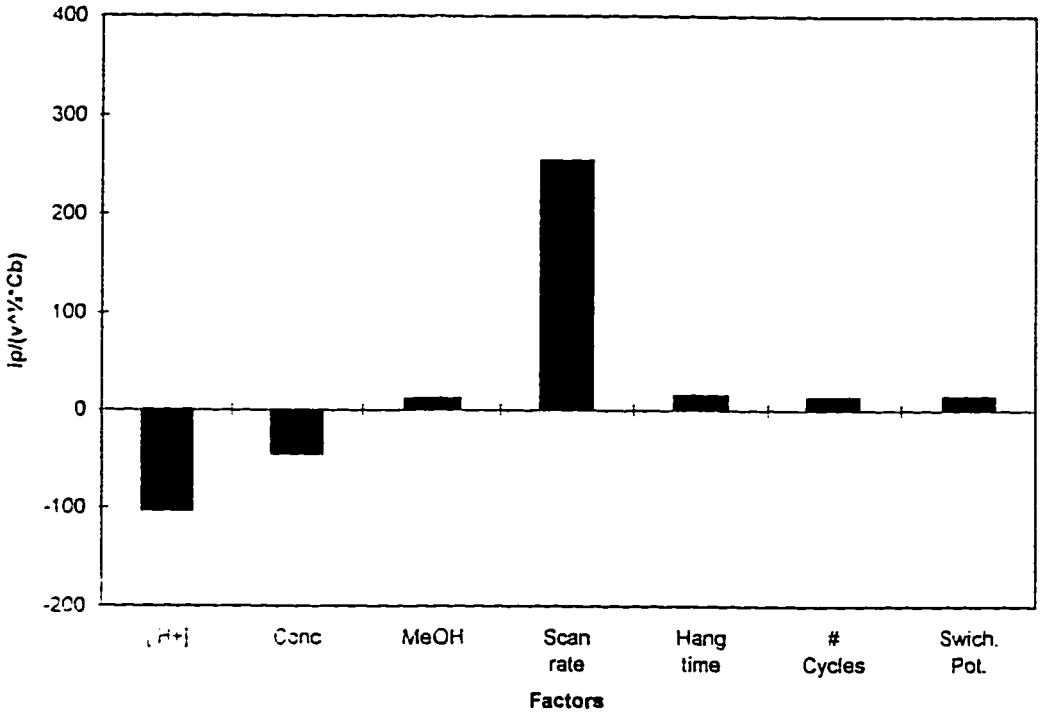

Figure 26. Calculated factor effects on the current function $i_p/ (v^{1/2} C^b)$ for peak B at pH 6 and pH 7 for the seven factors: pH, analyte concentration, methanol concentration, scan rate, hang time, number of cycles, and switching potential using experiments 1' - 4' and 5" - 8".

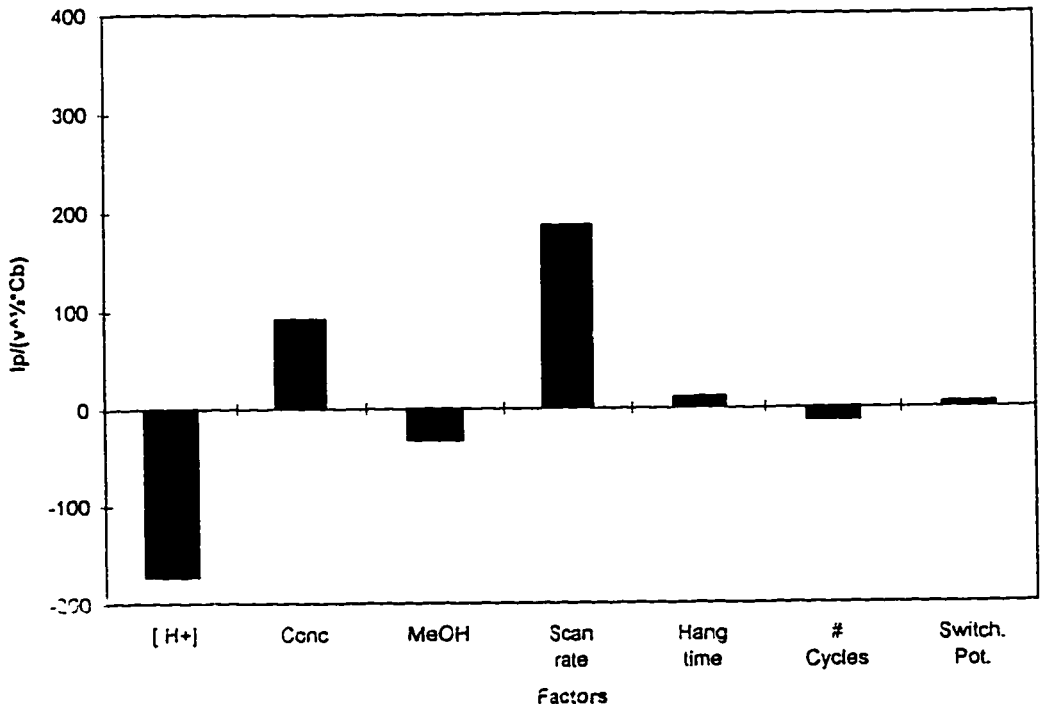

Figure 27. Calculated factor effects on current function $i_p/ (v^{½} C^{b})$ for peak A at pH 6 and pH 7 for the seven factors: pH, analyte concentration, methanol concentration, scan rate, hang time, number of cycles, and switching potential using experiments 1' - 4' and 5" - 8".

Scan rate was clearly a significant effect in all three cases. The effect of pH was also found to be significant in all three cases, however not nearly as significant as scan rate. Analyte and methanol concentration yielded values that gave inconsistent results either slightly higher or lower than the dummy variables. Hang time in all three cases did not exhibit a significant effect.

To calculate the significance of each of the factor effects a one sided F test was utilized (55). The observed variance in the experimental results was determined by use of two estimates of the variance: mean square error between levels (MSB) and mean square error within levels (MSE). To calculate MSB the following equation was utilized

$$MSB = N/4\ (\Delta^2) \tag{9}$$

where N is the total number of response values obtained in the experimental matrix and Δ is the difference between the average response at the low and high levels. MSE was calculated with

$$MSE = [\Sigma\ (n_r\text{-}1)\ (s_r^2)] / [\Sigma\ (n_r\text{-}1)] \tag{10}$$

where n_r is the number of response values per run and s_r is the sample variance for each run in the design matrix. The ratio of these two parameters yielded a value with an F distribution

$$MSB / MSE = F_o \tag{11}$$

where F_o is the observed ratio from the experimental data. The values for a one-tailed F test are denoted by $F(\alpha, \nu_1, \nu_2)$, where α is level of significance, ν_1 is numerator degrees of freedom, and ν_2 is the denominator degrees of freedom. For these data a level of

significance at the 95th percentile was chosen with 1 degree of freedom for the numerator and 6 degrees of freedom for the denominator. Using tables for percentiles of the F distribution (56), for F(.95, 1, 6) yielded a calculated value, $F_c = 5.99$.

Applying the F test to the current function factor effect for scan rate on peak B yielded the results shown in Table 15. The observed value for F_o is significantly greater than the calculated value, F_c of 5.99, thus it can be concluded that scan rate had a significant effect on the current function. In the same way the other six factors were subjected to the F test. A summary of the calculated F_o values for peak B at pH 7 and 11, peak B at pH 6 and 11 and peak A at pH 6 and 7 are found in Tables 16 - 18 respectively. As expected the two dummy variables yielded values that were not significant. Hang time in all three cases was not significant. Slightly higher, yet still not significant were the calculated F values for pH, analyte concentration and methanol concentration. Scan rate effect on the current function was significant for peak B but not peak A.

H. Effect of Variables

It was of interest to interpret the experimental design voltammetric data in order to gain insight into the electrochemical reaction mechanisms. Cyclic voltammetry is a useful analytical tool in this regard because it activates molecules by electron transfer and monitors the subsequent chemical reactions (57). In the following section, each of the seven variables will be considered in more depth.

Table 15. Calculating Significance of the Scan Rate Factor Effect on Current Function [$i_p/(v^{1/2} C^b)$] Based on Peak B Voltammetric Data for pH 7 and 11

Description		1000 mV/sec R(+)	250 mV/sec R(-)
Experiment	1'	424.4	-
	2'	379.2	-
	3'	-	102.0
	4'	-	101.9
	5'	497.5	-
	6'	453.5	-
	7'	-	156.5
	8'	-	99.5
Average		438.7	115.0
Grand Average			276.8
Delta Average.			323.7
Standard Deviation			27.7
(Std. Dev.)^2			768
M.S.B.			209531
M.S.E.			3244
F, observed			64.58
F, calculate (.95,1,6)			5.99
Significant? (Fo > Fc)			Yes

Table 16. F-test Results for Factor Effects on Current Function [$i_p/ (v^{1/2} C^b)$] Based on Peak B Voltammetric Data for pH 7 and 11, $F_c = 5.99$

Factor	F observed	F(.05; 1, 6)	Significant ?
pH	0.07	5.99	No
Analyte Concentration	0.02	5.99	No
Methanol Concentration	0.04	5.99	No
Scan Rate	64.58	5.99	Yes
Hang Time	0.001	5.99	No
Number of cycles *	0.006	5.99	No
Switching potential*	0.005	5.99	No

* = dummy variables

Table 17. F-test Results for Factor Effects on Current Function [$i_p/ (v^{1/2} C^b)$] Based on Peak B Voltammetric Data for pH 6 and 7, $F_c = 5.99$

Factor	F observed	F(.05; 1, 6)	Significant ?
pH	0.48	5.99	No
Analyte Concentration	0.08	5.99	No
Methanol Concentration	0.01	5.99	No
Scan Rate	13.30	5.99	Yes
Hang Time	0.006	5.99	No
Number of cycles *	0.010	5.99	No
Switching potential*	0.002	5.99	No

* = dummy variables

Table 18. F-test Results for Factor Effects on Current Function [$i_p/ (v^{1/2} C^b)$] Based on Peak A Voltammetric Data for pH 6 and 7, $F_c = 5.99$.

Factor	F observed	F(.05; 1, 6)	Significant ?
pH	2.04	5.99	No
Analyte Concentration	0.38	5.99	No
Methanol Concentration	0.05	5.99	No
Scan Rate	2.59	5.99	No
Hang Time	0.007	5.99	No
Number of cycles *	0.003	5.99	No
Switching potential*	0.003	5.99	No

* = dummy variables

1. Effect of Number of Cycles

For the previous analysis using the current function, **K** to calculate significant factor effects the voltammetric response of the second cycle in the voltammograms was not considered because this factor was used as a dummy variable. Yet, additional cycles of a voltammetric analysis can be informative if chemical reactions are coupled to the electron transfer (58). Figure 28 shows a representative two cycle voltammogram run under experiment 2' conditions. The second cycle exhibited decreased current response. It can be concluded that reaction products from the first scan are formed irreversibly (59, 60). All six experiments run with two cycles (2', 3', 5', 8', 5", and 8") exhibited lower currents for the second scan. In the case of experiment 5" and 8" run at pH 6 there was a significant shift in the peak potential of peak A for the second scan, see Figures 21 and 22. This was not observed for the four other two-cycle experiments run at pH 7 and 11.

2. Effect of Switching Potential

The timing of the switching potential was defined by either a 50 mV or 100 mV increment between the peak potential (PP) and the vertex 1 or switching potential (V1). This factor was also considered a dummy variable because the placement of the switching potential did not affect the character of the preceding portion of the voltammogram. If there had been an anodic peak measured on the reverse scan after the switching potential, this variable would likely have been influential. Shi and coworkers in a study of *p*-Nitrobenzoic acid showed that an anodic peak became lower as switching potential became more positive (61).

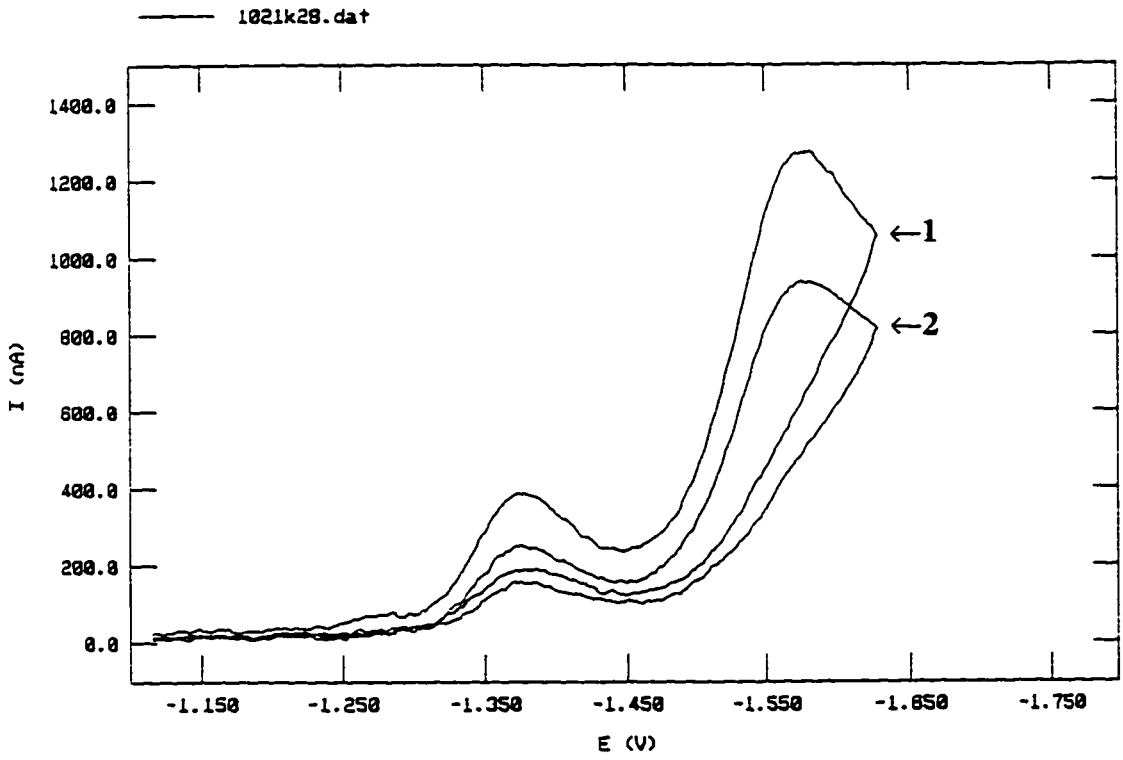

Figure 28. Ensemble-averaged, smoothed and blank corrected analyte cyclic voltammograms for experiment 2' with cycle number noted. Conditions in Table 3.

3. Effect of Drop Hang time

A hang time of either 1 or 30 seconds was selected to study the effect of solution equilibration time with a fresh mercury drop. The calculated F values for this variable yielded values as low as the two dummy variables, and so it can be concluded that hang time was not a significant effect. Because the solution equilibration takes place at a potential where no redox processes occur, this variable would only be expected to have an impact if low reactant adsorption were involved.

4. Effect of Analyte Concentration

In this study 0.1 mM and 0.5 mM ketorolac were used as the low and high values for the analyte concentration variable. In all three experimental sets the calculated F values demonstrated that this factor was not significant. It should not however be concluded that this electrochemical information is not analytically useful. Indeed, studies of other NSAIDs have shown that peak current varies linearly with concentration for: zomepirac (49), ketoprofen (50), and tolmetin (62, 63). Under similar conditions it is expected that ketorolac would behave similarly. However, for this work under the conditions investigated no significant change to the voltammetric current function was observed as analyte concentration was changed.

5. Effect of Methanol Concentration

A solvent that is to be used for electrochemical investigations should meet the following requirements: sufficiently soluble to the analyte, inert towards the electrolyte, possess as high a dielectric constant as possible [$\varepsilon_r > 10$], and be absent of impurities (64). Methanol, under the conditions used in this study, met all of these requirements. It was

soluble in the analyte and mixed readily in the buffer without reacting with it. Methanol has a dielectric constant of $\varepsilon_r = 32.66$ (65), so when used in the electrolyte it did not significantly decrease the conductivity of the solution. A high purity grade of methanol was utilized which contained low levels of impurities. This was confirmed when running a blank because no significant interferences were detected.

At the two levels of methanol investigated (2.5% and 10%), no significant effect was calculated for the current function. An additional series of experiments was conducted to focus on the effect of methanol on peak potential. Experiment 7' conditions were selected at pH 7 with methanol concentration varied from 2.5% to 10% . The voltammograms generated under these conditions yielded two cathodic peaks. The analyte and blank voltammograms were generated consecutively in the same day. Figure 29 shows blank corrected, smoothed voltammograms run at the two solvent concentrations. (Note: there is a higher level of noise exhibited here than in those previously shown because these voltammograms were not ensemble averaged.) Upon inspection of the voltammetric peak potentials for a representative set of three runs for the two conditions it was found that the average Peak A potentials did not differ more than the individual standard deviations. For the Peak B peak potentials with the use of a t test it can be concluded that there is no significant difference between these peak potentials at the 95% confidence limit, as shown in Table 19.

6. Effect of Scan Rate

From the calculations discussed previously it was shown that scan rate clearly had a significant effect on voltammetric current function. To further investigate the effect of

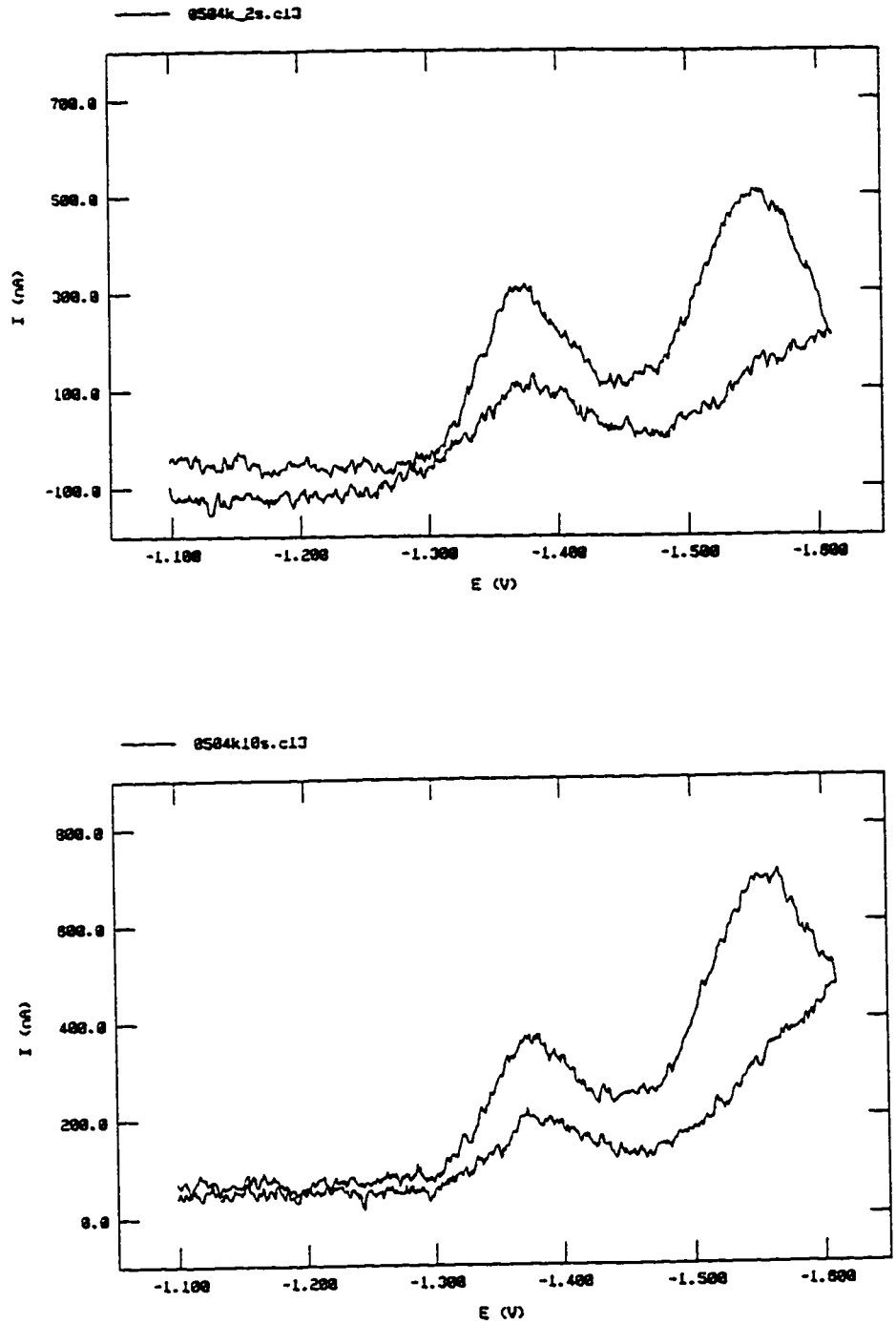

Figure 29. Smoothed and blank corrected analyte cyclic voltammograms varying methanol concentration for experiment 7' run at 2.5% methanol (A) and 10% methanol (B). Conditions in Table 3.

Table 19. Peak Potential E_p for Varying Methanol Concentrations

Methanol concentration (%)	**Peak A Potential E_p V**	**Peak B Potential E_p V**
2.5	-1.372	-1.546
2.5	-1.375	-1.549
2.5	-1.371	-1.552
Average	-1.373	-1.549
Std. Dev.	0.00208	0.00300
10.0	-1.379	-1.553
10.0	-1.374	-1.556
10.0	-1.378	-1.554
Average	-1.377	-1.554
Std. Dev.	0.00265	0.0153

Peak A does not differ more than individual standard deviations

F,observed for Peak B $F = (0.00300)^2 / (0.00153)^2 = 3.86$

F,calculated $F\ 0.05/2,2,2 = 39.00$

Pooled standard deviation, S_p

$$S_p = \{n\text{-}1(2.5\%)*[\text{std dev. } (10\%)]^2 + n\text{-}1\ (2.5\%)*[\text{std dev. } (10\%)]^2 / n(2.5\%)\text{-}1 + n(10\%)\ \text{-}1\}^{0.5}$$

$$S_p = \{(3\text{-}1)*[0.00300]^2 + (3\text{-}1)*(0.00153)^2 / (3\text{-}1) + (3\text{-}1)\}^{0.5}$$

$$S_p = 0.002381$$

$$t\ \text{observed} = \{[(\text{Avg. } 10\%) - (\text{Avg. } 2.5\%)] / Sp\} * \{[\ n(10\%)*\ n\ (2.5\%)] / \{[\ n(10\%) + n\ (2.5\%)]\}^{0.5}$$

$$t\ \text{observed} = [(-1.554) - (-1.549)] / 0.002381\ ] * \{[3*\ 3] / \{[3 + 3]\}^{0.5}$$

t observed = 2.56 t calculated = t 0.05/2,4 = 2.78

Conclusion: no significant difference between potentials at differing methanol concentrations for peak B

scan rate on peak potentials, a study was conducted using the experiment 7' conditions run at pH 7 with two different scan rates: 250 mV/sec and 1000 mV/sec. The Autoexecute feature of the electrochemical software permitted automated operation for alternating between the two scan rates for the same electrochemical cell. A test cell without analyte was run afterward in the same manner to blank correct the analyte voltammograms. The procedure involving alternating scan rates was applied to minimize the impact of any instrumental voltage drift.

For three replicate runs at the alternating scan rate a series of potential readings was collected as summarized in Table 20. A statistical treatment with the t test showed that there was a significant difference in peak potential for peak B at the 95% confidence limit. Peak A potentials did not differ more than the individual standard deviations at each scan rate. Figure 30 shows representative blank corrected and smoothed voltammograms collected at the two scan rates.

7. Effect of pH

To better understand the role that pH plays in the character of the voltammogram an additional series of experiments was conducted where pH was varied by individual pH units from pH 5 to pH 9. Experiment 7′ conditions were utilized: 0.1 mM analyte concentration, 2.5% methanol, 250 mV/sec scan rate, 1 cycle, 1 second hang time and 50 mV switching increment. It can be seen that pH of the solution has a significant effect on the voltammetric response as shown in Figure 31.

As pH was varied from pH 5 to pH 9 two opposing trends can be observed for the two cathodic peaks. Peak A at a potential of ~ -1.250 V was the only cathodic peak

Table 20. Peak Potential E_p for Varying Scan Rates

Scan rate (mV/sec)	Peak A Potential E_p (V)	Peak B Potential E_p (V)
250	-1.367	-1.560
250	-1.366	-1.557
250	-1.367	-1.557
Average	-1.367	-1.558
Std. Dev.	0.00058	0.0017
1000	-1.374	-1.574
1000	-1.367	-1.573
1000	-1.370	-1.573
Average	-1.370	-1.573
Std. Dev.	0.0035	0.00058

Peak A does not differ more that individual standard deviations

F,observed for Peak B $F = (0.00173)^2 / (0.00058)^2 = 9.00$

F,calculated F 0.05/2,2,2 = 39.00

Pooled standard deviation, S_p

$$S_p = \{n\text{-}1(250)*[\text{std. dev. } (250)]^2 + n\text{-}1\ (1000)*[\text{std. dev. } (1000)]^2 / n(250)\text{-}1 + n(1000)\ \text{-}1\}^{0.5}$$

$$S_p = \{(3\text{-}1)*[0.00058]^2 + (3\text{-}1)*(0.00173)^2 / (3\text{-}1) + (3\text{-}1)\}^{0.5}$$

$$S_p = 0.001290$$

$$t,\text{observed} = \{[(\text{Avg. } 1000) - (\text{Avg. } 250)] / Sp\} * \{[\ n(1000)*\ n\ (250)] / \{[\ n(1000) + n\ (250)]\}^{0.5}$$

$$t\ \text{observed} = [(-1.573) - (-1.558)] / 0.001290\ ] * \{[3*\ 3] / \{[3 + 3]\}^{0.5}$$

t observed = = 14.19

t calculated = t 0.05/2,4 = 2.78

Conclusion: significant difference between potentials at differing scan rates for peak B

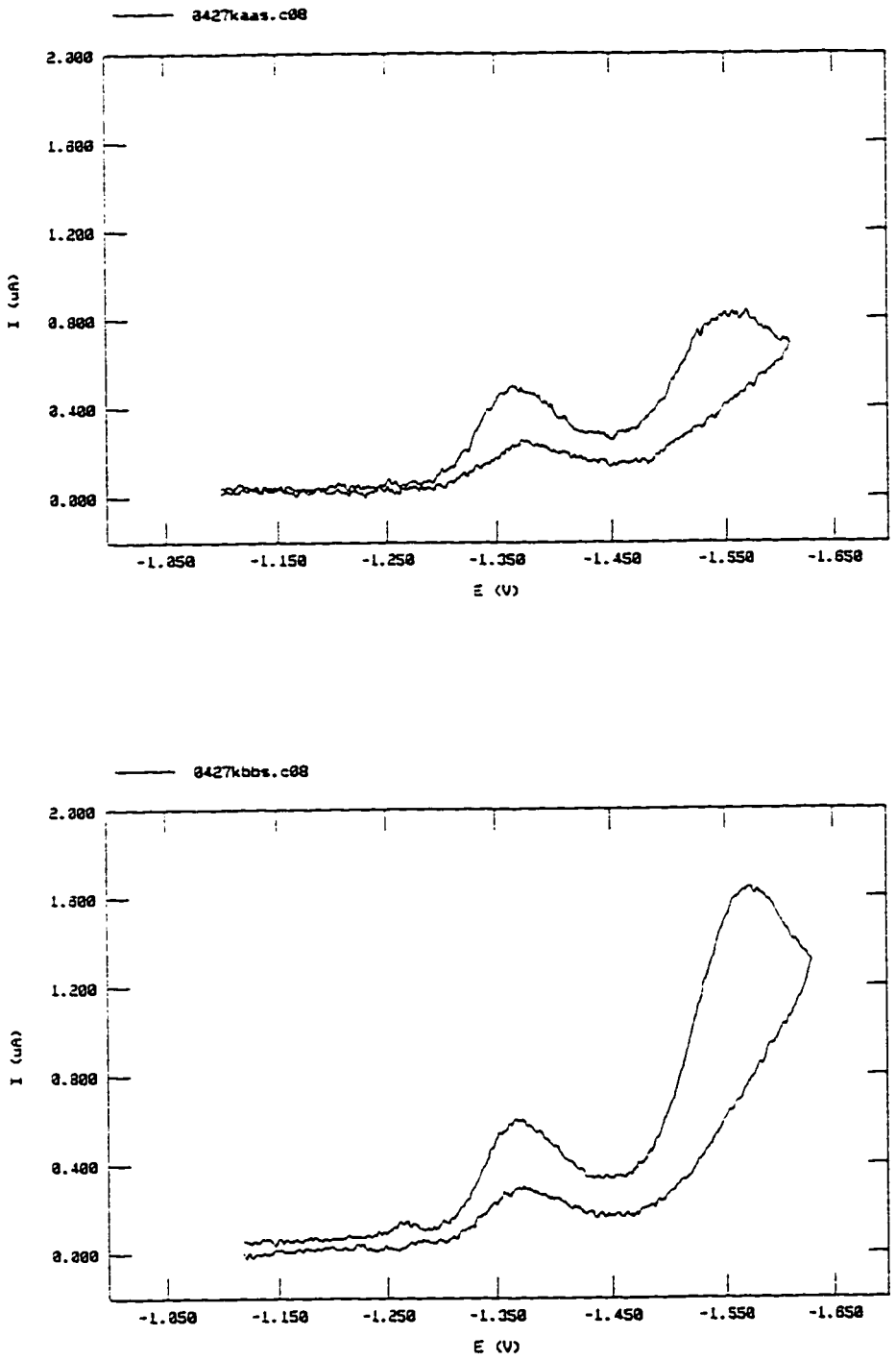

Figure 30. Smoothed and blank corrected analyte cyclic voltammograms varying scan rate for experiment 7' run at 250 mV/sec (A) and 1000 mV/sec (B). Conditions in Table 3.

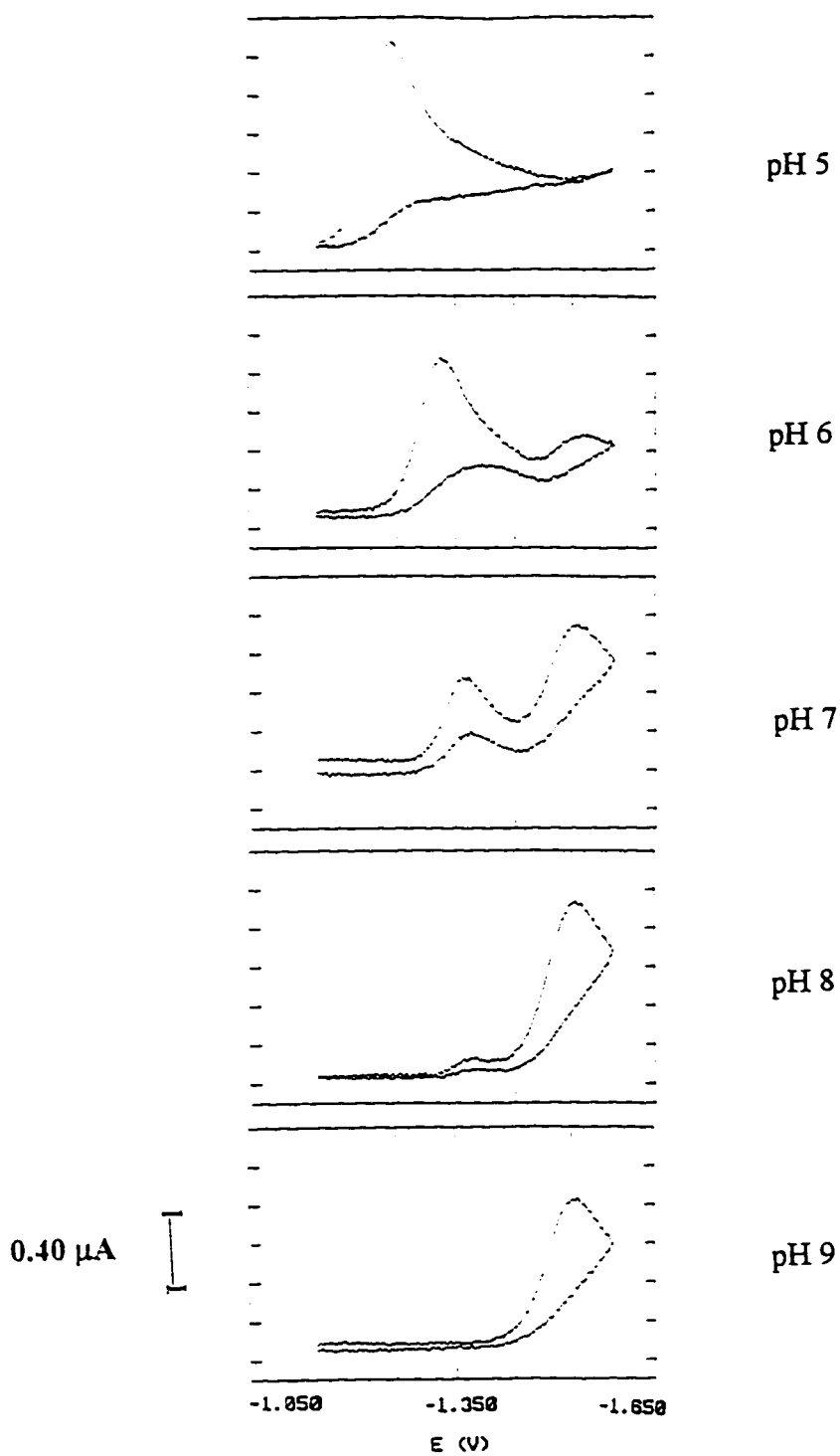

Figure 31. Effect of pH on voltammetric behavior using experiment 7' conditions (see Table 3). Voltammograms are blank-corrected for n=3.

observed at pH 5 and steadily diminished as pH was increased to pH 9. The opposite trend occurred for peak B, ~-1.550 V which was not detected at pH 5 and was found to steadily increase to pH 9. This can be better understood by plotting peak potentials E_p and peak current i_p for the two cathodic peaks as shown in Figures 32 and 33 respectively. A linear negative trend for peak current with pH is observed before it disappears at pH 9. The following equation fits this trend:

$$i_p \text{ (Peak A)} = -0.305 \text{ pH} + 2.597 \qquad r^2 = 0.9860 \qquad (12)$$

From Figure 28 the peak potential for peak A is clearly pH-dependent, moving more negative at ~ 60 mV/pH between pH 5 and 7. However, as was done for the scan rate and methanol variables, the effect of pH on peak potential was investigated by conducting a series of experiments where only pH was varied. Experiment 7′ conditions were utilized under conditions where both cathodic peaks were present. For this purpose pH 6 and pH 7 were selected. Figure 34 shows representative voltammograms. When using the t test it was concluded that both peaks showed a significant difference in potential as a result of pH change (see Tables 21 and 22).

I. Electrochemical Mechanism

By studying the electrochemical response information from this study as well as published work done with similar compounds it is possible to suggest explanations for the electrochemical behavior of ketorolac. One study of interest for this work was conducted by Chatten et al. in which zomepirac, a structurally similar NSAID (see Figure 1C), was investigated (66). Using NMR and IR coupled to electrochemical techniques it was concluded that the carbonyl group was the site of the reduction process. Applying the

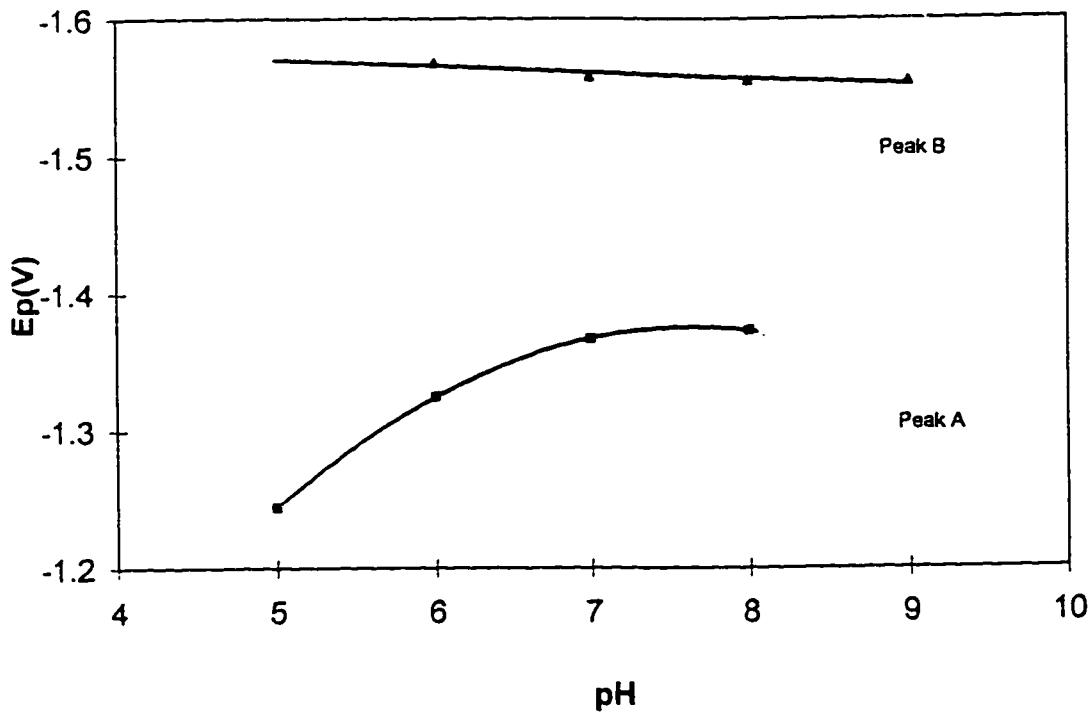

Figure 32. Effect of pH on the peak potential E_p for ketorolac voltammetric data using experiment 7' conditions (see Table 3).

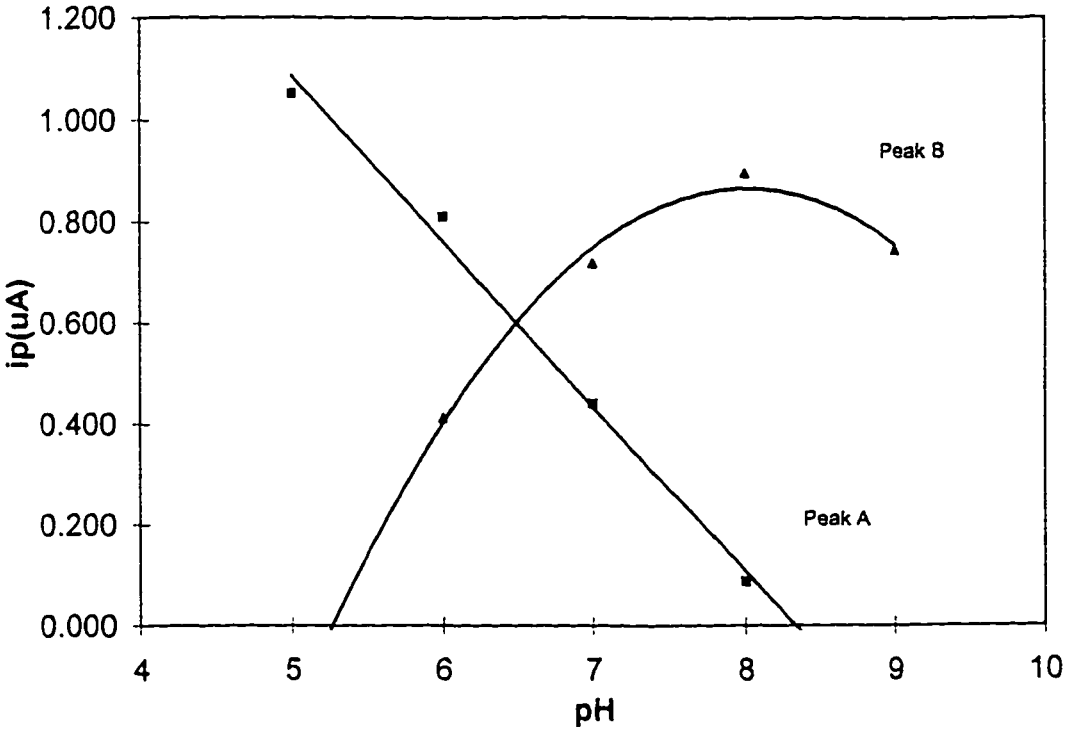

Figure 33. Effect of pH on the peak current i_p for ketorolac voltammetric data using experiment 7' conditions (see Table 3).

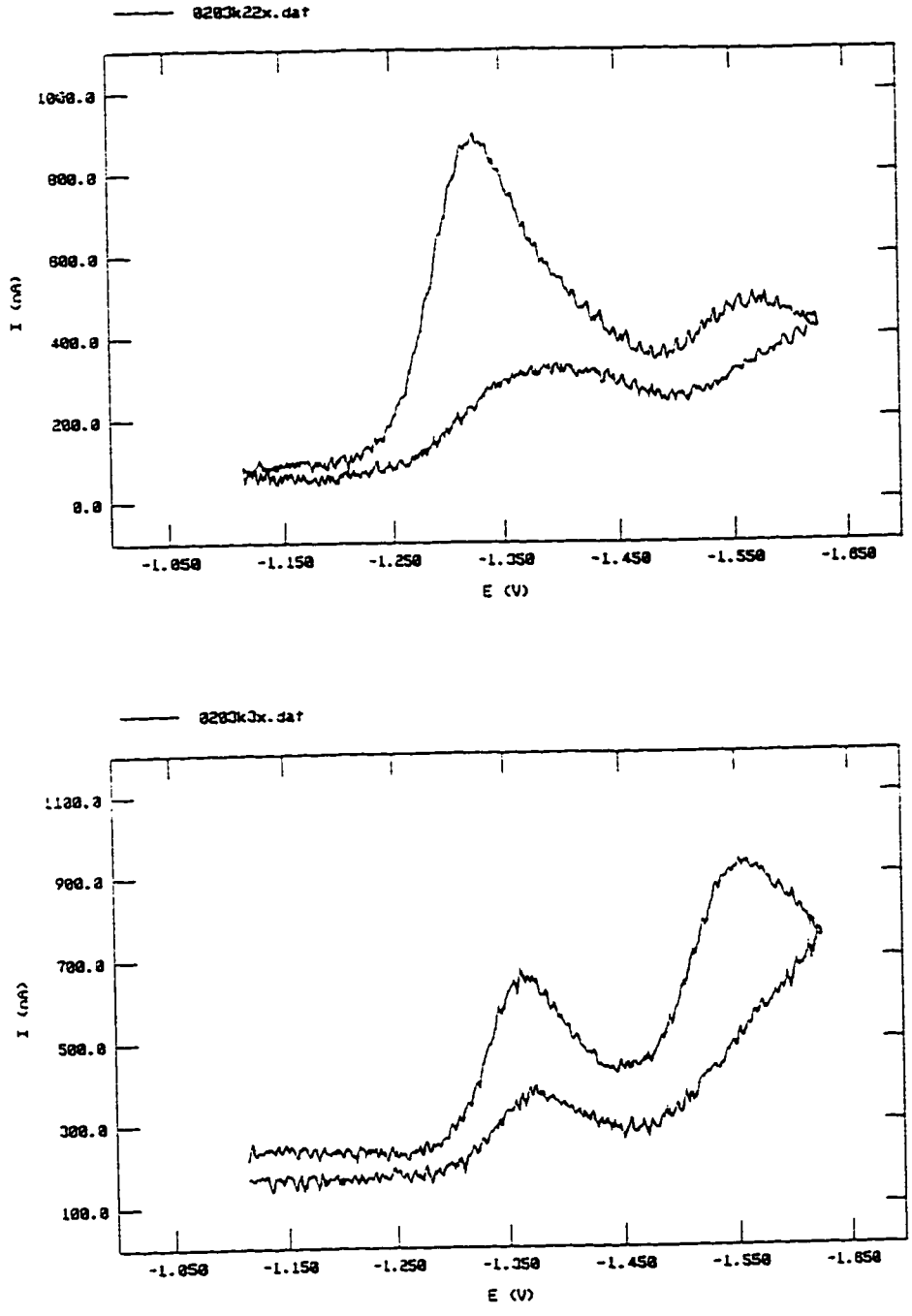

Figure 34. Smoothed and blank corrected analyte cyclic voltammograms varying pH for experiment 7' run at pH 6 (A) and pH 7 (B). Conditions in Table 3.

Table 21. Peak Potential E_p for Varying pH for Peak A

pH	Peak A Potential E_p V
6	-1.330
6	-1.326
6	-1.329
Average	-1.328
Std. Dev.	0.00208
7	-1.370
7	-1.368
7	-1.367
Average	-1.368
Std. Dev.	0.00153

F,observed for Peak A $F = (0.00208)^2 / (0.00153)^2 = 1.86$

F,calculated $F\ 0.05/2,2,2 = 39.00$

Pooled standard deviation, S_p

$$S_p = \{n\text{-}1(pH6)*[\text{std dev }(pH6)]^2 + n\text{-}1\ (pH7)*[\text{std dev }(pH7)]^2 / n(pH6)\text{-}1 + n(pH7)\ \text{-}1\}^{0.5}$$

$$S_p = \{(3\text{-}1)*[0.00208]^2 + (3\text{-}1)*(0.00153)^2 / (3\text{-}1) + (3\text{-}1)\}^{0.5}$$

$$S_p = 0.001826$$

$$\text{t observed} = \{[(\text{Avg. pH7}) - (\text{Avg. pH6})] / Sp\} * \{[\ n(pH6)*\ n\ (pH7)] / \{[\ n(pH6) + n\ (pH7)]\}^{0.5}$$

$$\text{t observed} = [(-1.368) - (-1.328)] / 0.001826\ ] * \{[3*\ 3] / \{[3 + 3]\}^{0.5}$$

$$\text{t observed} = = 26.73$$

$$\text{t calculated} = t\ 0.05/2,4 = 2.78$$

Conclusion: significant difference between potentials at varying pH for peak A

Table 22. Peak Potential E_p for Varying pH for Peak B

pH	Peak B Potential E_p V
6	-1.565
6	-1.571
6	-1.575
Average	-1.570
Std. Dev.	0.00503
7	-1.558
7	-1.558
7	-1.560
Average	-1.559
Std. Dev.	0.00115

F,observed for Peak B $F = (0.00503)^2 / (0.0115)^2 = 19.13$

F,calculated F 0.05/2,2,2 = 39.00

Pooled standard deviation, S_p

$$S_p = \{n\text{-}1(pH6)*[\text{std dev } (pH6)]^2 + n\text{-}1\ (pH7)*[\text{std dev } (pH7)]^2 / n(pH6)\text{-}1 + n(pH7)\ \text{-}1\}^{0.5}$$

$$S_p = \{(3\text{-}1)*[0.00503]^2 + (3\text{-}1)*(0.00115)^2 / (3\text{-}1) + (3\text{-}1)\}^{0.5}$$

$$S_p = 0.003649$$

$$\text{t observed} = \{[(\text{Avg. } pH7) - (\text{Avg. } pH6)] / Sp\} * \{[\ n(pH6)*\ n\ (pH7)] / \{[\ n(pH6) + n\ (pH7)]\}^{0.5}$$

$$\text{t observed} = [(-1.570) - (-1.559)] / 0.003649\ ] * \{[3*\ 3] / \{[3 + 3]\}^{0.5}$$

t observed = = 3.68

t calculated = t 0.05/2,4 = 2.78

Conclusion: significant difference between potentials at varying pH for peak B

reduction pathway that was proposed for zomepirac to ketorolac results in an irreversible two-electron process that is illustrated in Figure 35. The first step in this proposed scheme is the reduction of the keto group by a one electron process to yield a free radical anion. This anion is probably in rapid equilibrium with the protonated radical, consistent with the pH dependence of peak A. The failure to observe a reverse anodic peak for peak A suggests there is a rapid irreversible dimerization of the radical (67). At the more negative potential the radical anion undergoes an additional one-electron reduction to form the dianion. In acidic conditions, this compound becomes protonated to give the alcohol.

This scheme, in which there are two subsequent one-electron reactions, each followed by an irreversible reaction, finds support in the experimental results of this study. Cathodic peaks A and B can be attributed to the first and second reduction steps respectively. The large scan rate effect on the current functions for both peaks strongly suggests that surface adsorption is involved in the electrode processes. The observation of a negative-going peak on the reverse sweep at about the potential of peak A (see Figure 31) is very unusual, but would be consistent with potential-dependent desorption of an insulating product, allowing renewed reduction of analyte which had been somewhat inhibited by product buildup at more negative potentials. Because it was not the primary objective of this work to elucidate in detail the overall electrode process, no further studies were performed to refine the mechanistic observations included here.

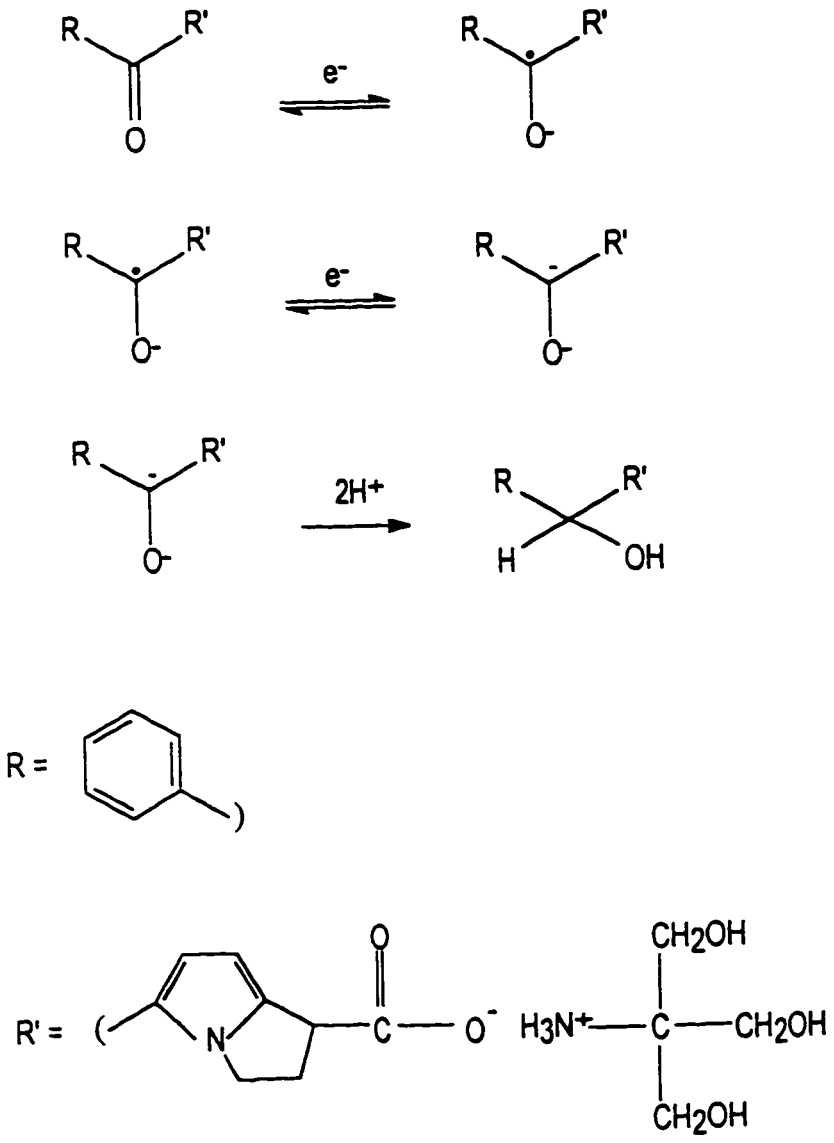

Figure 35. Proposed mechanism for the reduction of ketorolac tromethamine based on reference 67.

VI. Summary

A set of optimized experimental conditions was established for the electrochemical study of ketorolac. A static mercury drop electrode with a Britton-Robinson buffer as the supporting electrolyte was employed. To correct for *iR* drop a positive feedback algorithm in the PAR EG&G software was utilized. Voltammetric signal-to-noise was significantly enhanced with the use of ensemble averaging and a Savitzky-Golay smoothing routine.

Experimental variables that affected voltammetric response were studied by means of a Plackett-Burman fractional factorial experimental design. This design allowed the evaluation of seven experimental variables: pH, analyte concentration, methanol concentration, scan rate, number of cycles, hang time, and switching potential with a minimum number of experiments. The voltammetric current function, $i_p/ (v^{½} C^b)$, was chosen as the primary figure of merit with which to evaluate the voltammetric data for each cathodic peak. By means of statistical tests it was determined that scan rate had the only significant effect on the current function for each peak.

The effect of some experimental factors (scan rate and pH) on cathodic peak potential was also investigated. It was found that varying scan rate from 250 to 1000 mV/sec significantly affected the potential of peak B but not peak A. When varying pH from pH 6 to pH 7 it was found that there was a significant difference in potential of both peaks A and B.

Further investigations of each of the variables gave insight into the mechanism of ketorolac. There was good evidence that both cathodic peaks were affected by adsorption

processes. Under acidic conditions a reduction peak was observed in the anodic sweep, possibly due to potential-dependent desorption of an insulting reduction product.

VII. Conclusions

These results demonstrate a useful experimental approach for acquiring meaningful voltammetric data from an electrochemically active pharmaceutical compound. It was shown that the voltammetric current and potential information related to multiple experimental variables in an efficient factorial design can provide a multivariate perspective on redox behavior. Further study for this work will involve comparing these experimental results with other related pharmaceutical compounds. It would be worthwhile to look for correlations in the voltammetric data gathered with biological activity measurements. It is envisioned that the experimental protocol developed in this study could have future application as a screening tool for the presence of pharmaceutical activity.

VIII. Bibliography

1. Lee, C. *Development and Evaluation of Drugs*; CRC: Boca Raton, 1993; pp 21-22.

2. Smith, C. G. *The Process of New Drug Discovery and Development*; CRC: Boca Raton, 1992; p 139.

3. Patriarche, G. J.; Vire, J-C.; Kaufmann, J.-M. *Anal. Proc.* **1985**, *22*, 202-203.

4. Chatten, L.G. *J. Pharm. Biomed. Anal.* **1983**, *1*, 491-495.

5. Chatten, L. G. *Acta Pharma. Jugosl.* **1990**, *40*, 159-169.

6. DePalma, R. A.; Perone, S. P. *Anal. Chem.* **1979**, *51*, 825-828.

7. Schachterle, S. D.; Perone, S. P. *Anal. Chem.* **1981**, *53*, 1672-1677.

8. Byers, W. A.; Freiser, B. S.; Perone, S. P. *Anal. Chem.* **1983**, *55*, 620-625.

9. Nelson, P.H. In *CRC Handbook of Eicosanoids; Prostaglandins and Lipids. Vol. 11. Drugs Acting via the Eicosanoids;* Willis, A. L., Ed.; CRC: Boca Raton, 1989; pp 59-64.

10. *Physicians Desk Reference*; E. R. Barnhart, publisher, Medical Economics: Oradell, New Jersey, 1988 p 2213.

11. Muller, F. O.; Gosling, J. A.; Erdmann, G. H. *South African Med. J.* **1977**, *51*, 794-796.

12. Kaplan, S.; Salzman, R. *Curr. Therap. Res.* **1979**, *25*, 508-518.

13. *Physicians Desk Reference*; E. R. Barnhart, publisher, Medical Economics: Oradell, New Jersey, 1988 p 2090.

14. O'Hara, D. A.; Fragen, R. J.; Kinzer, M.; Pemberton, D. *Clin. Pharmacol. Ther.* **1987**; *41*, 556-561.

15. Yee, J.; Brown, C. R.; Sevelius, H.; Wild, V. *Clin. Pharmacol. Ther.* **1985**, 37, 215.

16. Muchowski, J. M.; Unger, S. H.; Ackrell, J.; Cheung, P.; Cooper, G. F.; Cook, J.; Gallegra, P.; Halpern, O.; Koehler, R.; Kluge, A. F.; Van Horne A. R.; Antonio, Y.; Carpio, H.; Franco, F.; Galeazzi, E.; Garcia, I.; Greenhouse, R.; Guzmán, A.; Irarte, J.; Leon, A.; Peña, A.; Peréz, V.; Valdéz, D.; Ackerman, N.; Ballaron, S. A.; Krishna Murthy D. V.; Rovito J. R.; Tomolonis, A. J.; Young, J. M.; Rooks II, W. H. *J. Med. Chem.* **1985**, *28*, 1037-1049.

17. Muchowski, J. M.; Cooper, G. F.; Halpern, O.; Koehler, R.; Kluge, A. F.; Simon, R. L.; Unger, S. H.; Van Horne A. R.; Wren, D. L.; Ackrell, J.; Antonio, Y.; Franco, F.; Greenhouse, R.; Guzmán, A.; Leon, A.; Ackerman, N.; Ballaron, S. A.; Krishna Murthy D. V.; Rovito J. R.; Tomolonis, A. J.; Young, J. M.; Rooks II, W. H. *J. Med Chem.* **1987**, *30*, 820-823.

18. Dunn, J. P.; Green, D. M.; Nelson, P. H.; Rooks, W. H.; Tomolnois, A.; Untec, K. G. *J. Med. Chem.* **1977**, *20*, 1557.

19. Ackrell, J.; Antonio, Y.; Franco, F.; Landeros, R.; Leon, A.; Muchowski, J. M.; Maddox, M. L.; Nelson, P. H.; Rooks, W. H.; Roszkowski, A. P.; Wallach, M. B. *J. Med. Chem.* **1978**, *21*, 1035.

20. Dunn, J. P.; Muchowski, J. M.; Nelson , P. H. *J. Med. Chem.* **1981**, *24*, 1097.

21. Rooks, W. H.; Tomolonis, A. J.; Maloney, P. J.; Roszkowski, A. P.; Wallach, M. B. *Agents Action* **1980**, *10*, 266.

22. Vane, J. R.; *Nature* **1971**, *231*, 232.

23. Bohinski, R. C. *Modern Concepts in Biochemistry*; Allyn and Bacon: Boston, 1983; p 228.

24. Shen, T. Y., *Non-Steroidal Anti-inflammatory Drugs;* Garattini, S., Dukes, M. N. G.; Eds., Excerpta Medica Foundation: Milan, 1964; p 13.

25. Gund, P.; Shen T.Y. *J. Med. Chem.* **1977**, *20*, 1148.

26. Nelson, P.H. In *CRC Handbook of Eicosanoids; Prostaglandins and Lipids. Vol. 11. Drugs Acting via the Eicosanoids;* Willis, A. L., Ed.; CRC: Boca Raton, 1989; p 65.

27. Buckley, M. M. T.; Brogden, R. N. *Drugs* **1990**, *39*, 86.

28. Gund, P.; Shen T.Y. *J. Med. Chem.* **1977**, *20*, 1146-1152.

29. Peterson, W. M. *Am. Lab* **1979**, *11*, 69.

30. Bard, A. J.; Faulkner, L. R. *Electrochemical Methods*; Wiley: New York, 1980; p 22.

31. Technical Note No. 101; EG&G Princeton Applied Research: Princeton, NJ, 1986.

32. *Model 270/250 Research Electrochemistry Software User's Guide*; EG&G Princeton Applied Research: Princeton, NJ, 1992; p 124.

33. Bard, A. J.; Faulkner, L.R. *Electrochemical Methods*; Wiley: New York, 1980; p 215.

34. Skoog, D. A. *Principles of Instrumental Analysis*; Saunders College: Philadelphia, 1985; p 688.

35. Gosser, D. K. *Cyclic Voltammetry: Simulation and Analysis of Reaction Mechanisms*; VCH: New York, 1993; p 27.

36. Hieftje, G. M. *Anal. Chem.* **1972**, *44* (7), 69A-78A.

37. Rowell, R. L. *J. Chem. Educ.* **1975**, *47*, 24A.

38. Savitzky, A.; Golay, M. *Anal. Chem.* **1964**, *36*, 1627-1639.

39. Schibler, J. A.; Fan, D.; Gragg, D. Presented at the 47th Pittsburgh Conference on Analytical Chemistry and Applied Spectroscopy, Chicago, IL, March 1996; Paper 1337.

40. Byers, W. A.; Perone, S. P. *Anal. Chem.* **1983**, *55*, 616.

41. Vindevogel, J.; Sandra, P. *Anal. Chem.* **1991**, *63*, 1531.

42. Schmidt, S. R.; Launsby, R. J. *Understanding Industrial Designed Experiments*; Air Academy: Colorado Springs, 1992; p (1-36).

43. Plackett, R. C.; Burman, J. P. *Biometrica*, **1946**, *23*, 305.

44. Montgomery, D. C. *Design and Analysis of Experiments*; John Wiley & Sons: New York, 1991; p 244.

45. *Model 270/250 Research Electrochemistry Software User's Guide*; EG&G Princeton Applied Research: Princeton, NJ, 1992; pp 123-188.

46. Reference 45 pp 73-80.

47. Byers, W. A.; Freiser, B. S.; Perone, S. P. *Anal. Chem.* **1983**, *55*, 621.

48. Hary, D.; Jaffe, M. B. *Sci. Comput. Auto.* **1994**, *11* (6),18.

49. Chatten, L.G.; Pons, S.; Amankwa, L. *Analyst* **1983**, *108*, 998.

50. Amankwa, L.; Chatten, L.G. *Analyst* **1984**, *109*, 59.

51. Wandlowski, T.; Gosser, D.; Akinele, R.; De Levie, R.; Horvak, V. *Talanta* **1993**, *40* 1792.

52. Frazer, J. W.; Carlson, L. R.; Kray, A. M.; Bertoglio, M. R.; Perone, S. P. *Anal. Chem.* **1971**, *43*, 1485-1490.

53. Heineman, W. R.; Kissinger, P. T. In *Laboratory Techniques in Electroanlyatical Chemistry*; Kissinger, P. T.; Heineman, W. R., Eds. Marcel Dekker: New York, 1984; p. 82.

54. Vindevogel, J.; Sandra, P. *Anal. Chem.* **1991**, *63*, 1530.

55. Schmidt, S. R.; Launsby R. J. *Understanding Industrial Designed Experiments*, Air Academy: Colorado Springs, 1992; pp (4-1)-(4-10).

56. Anderson, R. L *Practical Statistics for Analytical Chemists*; Van Nostrand Reinhold: New York, 1987; pp 289-295.

57. Gosser, D. K. Jr. *Cyclic Voltammetry: Simulation and Analysis of Reaction Mechanisims*; VCH: New York, 1993; p vii.

58. Reference 57 p 42.

59. Setiadji, R.; Wang, J.; Santana-Rios, G. *Talanta* **1993**, *40*, 846.

60. Gomez de Balugera, Z.; Barrio, R.J.; Goicolea, A.; Arranz, J.F *Electroanalysis* **1991**, *3*, 425.

61. Shi, C.; Zhang, W.; Birke, R. L.; Gosser, D. K. Jr.; Lombardi, J. R. *J. Phys. Chem.* **1991**, *95*, 6278.

62. Hagga, M. E. M.; Abounassif, MA.; Dawoud, A.H.; Pakistan *J. Pharm. Sci.*, **1991**, 4, 1-9.

63. Al-Khamees, H. A.; Al-Obaid, A.M.; Al-Rashood, K.A.; Bayomi, S.M.; Mohamed, M.E. *J. Pharm. Bio. Anal.* **1990**, *8*, 225-228.

64. Reichardt, R. *Solvent and Solvent Effects in Organic Chemistry*; VCH: New York, 1990; pp 430-431.

65. Reference 64 p 408.

66. Chatten, L.G.; Pons, S.; Amankwa, L. *Analyst* **1983**, *108*, 1000.

67. Reference 66 p 999.